REPORT OCEANOGRAPHY No.. 47, 2013

Evaluation of the SMHI coupled atmosphere-ice-ocean model RCA4-NEMO

C. Dieterich, S. Schimanke, S. Wang, G. Väli, Y. Liu, R. Hordoir, L. Axell, A. Höglund, H.E.M. Meier

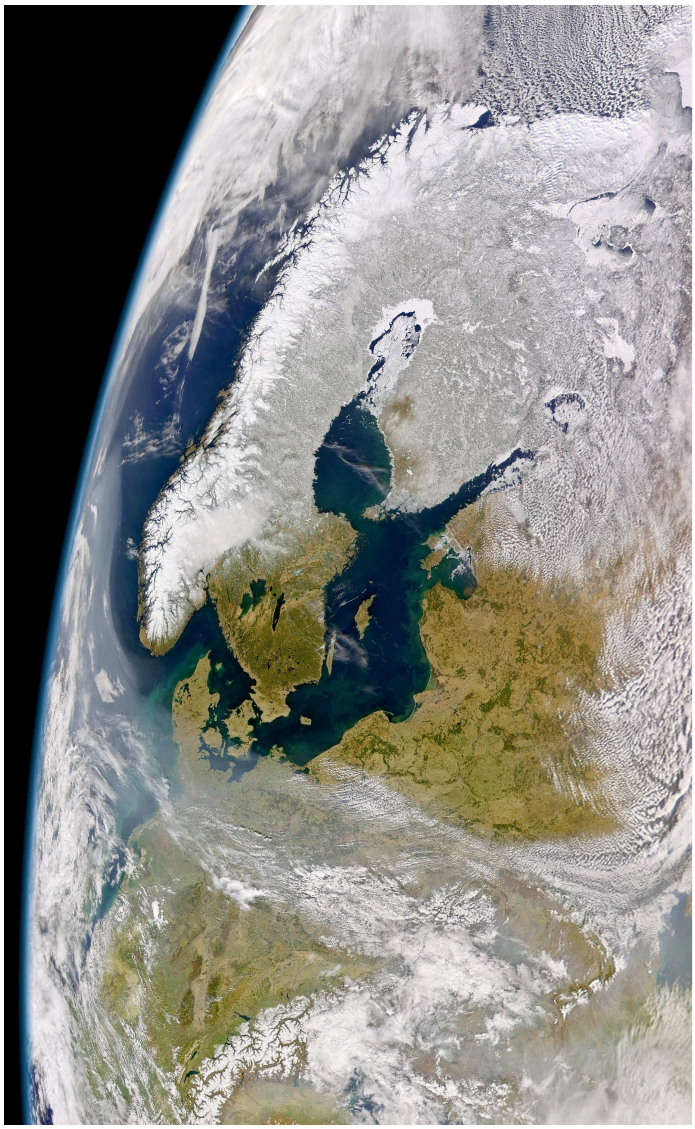

Front:
The North Sea and Baltic Sea region in the foreground as part of the global climate system. This SeaWiFS picture illustrates the different model components of the coupled atmosphere-ice-ocean model RCA4-NEMO. Image courtesy the SeaWiFS Project, NASA/Goddard Space Flight Center and ORBIMAGE.

ISSN: 0283-1112

REPORT OCEANOGRAPHY No. 47, 2013

Evaluation of the SMHI coupled atmosphere-ice-ocean model RCA4-NEMO

C. Dieterich, S. Schimanke, S. Wang, G. Väli, Y. Liu, R. Hordoir, L. Axell, A. Höglund, H.E.M. Meier

Report Summary / Rapportsammanfattning

Issuing Agency/Utgivare	Report number/Publikation
Swedish Meteorological and Hydrological Institute SE - 601 76 NORRKÖPING Sweden	Report Oceanography 47
	Report date/Utgivningsdatum February 2013

Author (s)/Författare

C. Dieterich, S. Schimanke, S. Wang, G. Väli, Y. Liu, R. Hordoir, L. Axell, A. Höglund, H.E.M Meier

Title (and Subtitle/Titel

Evaluation of the SMHI coupled atmosphere-ice-ocean model RCA4-NEMO

Abstract/Sammandrag

The regional, coupled atmosphere-ice-ocean model RCA4-NEMO developed at the SMHI is evaluated on the basis of an ERA40 hindcast. While the development of the regional climate model is continuing a first assessment is presented here to allow for an orientation about the status quo. RCA4-NEMO in its present form consists of two model components. The regional atmosphere model RCA4 covers the whole of Europe and is interactively coupled to a North Sea and Baltic Sea ice-ocean model based on NEMO. RCA4-NEMO is currently being used to downscale CMIP5 scenarios for the North Sea and Baltic Sea region for this century. As a part of the validation of RCA4-NEMO we present an analysis and discussion of the hindcast period 1970 - 1999. The model realization is compared to observational records. Near surface temperatures and heat fluxes compare reasonably well with records of in-situ measurements and satellite derived estimates. For salinities and freshwater fluxes the agreement with observations is not satisfactory yet. The momentum fluxes transferred from the atmosphere to the ice-ocean model are identified as one of the sensitive processes in the coupling of both model components. Except for the freshwater exchange between atmosphere and ocean the climatological near surface properties and corresponding fluxes compare well with climatological estimates for the period 1970 – 1999.

Den regionala kopplade atmosfär-is-havsmodellen RCA4-NEMO, som utvecklats vid SMHI, utvärderas baserat på en ERA40-återanalys. Utvecklingen av den regionala klimatmodellen fortsätter men en första utvärdering presenteras här för att informera om aktuell status. RCA4-NEMO i aktuell status innehåller två modell komponenter. Den regionala atmosfärmodellen RCA4 täcker hela Europa och är tvåvägskopplad till en is-hav-modell för Nordsjön och Östersjön baserat på NEMO. Den används för tillfället för nedskalning av CMIP5-scenarier för detta århundrade för Nordsjön och Östersjön. Som en del av utvärderingen av RCA4-NEMO presenteras en analys och diskussion av hindcast-körning 1970 - 1999. Modellresultaten jämförs med observationsdata. Temperatur nära ytan och värmeflödet är förhållandevis bra vid en jämförelse med in-situ-mätningar och skattningar baserade på satellitdata. Salthalt och färskvattenutbyte är dock mindre bra. Momentumflödet från atmosfär till hav identifieras som en kritisk process i kopplingen mellan modellerna. Med undantag för färskvattensutbytet mellan atmosfär och hav är de klimatologiska egenskaperna nära ytan och motsvarande flöden jämförbara med klimatologiska observationer för perioden 1970 - 1999.

Key words/sök-, nyckelord

RCA4-NEMO, coupled, regional, climate, atmosphere-ice-ocean, model, RCM, North Sea, Baltic Sea, ERA40, hindcast, simulation, evaluation

Supplementary notes/Tillägg	Number of pages/Antal sidor	Language/Språk
	60	English

ISSN and title/ISSN och titel

0283-1112 Report oceanography

Report available from/Rapporten kan köpas från:

SMHI
SE - 601 76 NORRKÖPING
Sweden

Summary

The regional, coupled atmosphere-ice-ocean model RCA4-NEMO developed at the SMHI is evaluated on the basis of an ERA40 hindcast. While the development of the regional climate model is continuing a first assessment is presented here to allow for an orientation about the status quo. RCA4-NEMO in its present form consists of two model components. The regional atmosphere model RCA4 covers the whole of Europe and is interactively coupled to a North Sea and Baltic Sea ice-ocean model based on NEMO. RCA4-NEMO is currently being used to downscale CMIP5 scenarios for the North Sea and Baltic Sea region for this century. As a part of the validation of RCA4-NEMO we present an analysis and discussion of the hindcast period 1970 - 1999. The model realization is compared to observational records. Near surface temperatures and heat fluxes compare reasonably well with records of in-situ measurements and satellite derived estimates. For salinities and freshwater fluxes the agreement with observations is not satisfactory yet. The momentum fluxes transferred from the atmosphere to the ice-ocean model are identified as one of the sensitive processes in the coupling of both model components. Except for the freshwater exchange between atmosphere and ocean the climatological near surface properties and corresponding fluxes compare well with climatological estimates for the period 1970 - 1999.

Sammanfattning

Den regionala kopplade atmosfär-is-havsmodellen RCA4-NEMO, som utvecklats vid SMHI, utvärderas baserat på en ERA40-återanalys. Utvecklingen av den regionala klimatmodellen fortsätter men en första utvärdering presenteras här för att informera om aktuell status. RCA4-NEMO i aktuell status innehåller två modell komponenter. Den regionala atmosfärmodellen RCA4 täcker hela Europa och är tvåvägskopplad till en is-hav-modell för Nordsjön och Östersjön baserat på NEMO. Den används för tillfället för nedskalning av CMIP5-scenarier för detta århundrade för Nordsjön och Östersjön. Som en del av utvärderingen av RCA4-NEMO presenteras en analys och diskussion av hindcast-körning 1970 - 1999. Modellresultaten jämförs med observationsdata. Temperatur nära ytan och värmeflödet är förhållandevis bra vid en jämförelse med in-situ-mätningar och skattningar baserade på satellitdata. Salthalt och färskvattenutbyte är dock mindre bra. Momentumflödet från atmosfär till hav identifieras som en kritisk process i kopplingen mellan modellerna. Med undantag för färskvattensutbytet mellan atmosfär och hav är de klimatologiska egenskaperna nära ytan och motsvarande flöden jämförbara med klimatologiska observationer för perioden 1970 - 1999.

Contents

1 Introduction

During the past fifteen years several regional climate models have been developed for the North Sea and Baltic Sea region [*Tian et al.*, 2013; *Ho et al.*, 2012; *Schrum et al.*, 2003; *Döscher et al.*, 2002; *Hagedorn et al.*, 2000; *Gustafsson et al.*, 1998]. Since the region of the North Sea and Baltic Sea is usually not well represented neither in global atmosphere and even less so in global ocean models there is a demand for regional models with a much higher resolution. The higher resolution allows for a better representation of crucial processes and relevant topographic features. On the other hand the higher resolution renders the numerical models too bulky to run them on a global grid. A classical approach is to use regional models that use information about the world outside the model domain by means of open boundaries.

That establishes the prerequisite to integrate the regional climate models (RCMs) for long time scales. One specific application on this backdrop is the downscaling of scenarios produced by global climate models (GCMs). This enables the investigation of regional trends, extreme events and other statistical properties of climate for the next couple of decades. It is well known that for example the Arctic Amplification of climate change is due to specific processes like ice-albedo feedback [*Curry et al.*, 1995]. To be able to tell sensible processes on a regional scale from those that are less prone to changes of the large scale climate it is necessary to resolve those processes. For the example of the Arctic Amplification the processes that need to be resolved are the ice cover and its seasonal cycle [*Robock*, 1980].

For the North Sea and Baltic Sea region the interaction with the complicated geography and topography is one reason to expect that atmospheric and oceanic circulation can be improved by adding resolution to a coupled atmosphere-ice-ocean model. The pattern of large scale rainfall is strongly influenced by mountain ranges. For instance, the geographical distribution of precipitation is better captured in an RCM than in ERA40 which is mainly a consequence of a higher resolution [*Samuelsson et al.*, 2011]. For the ocean circulation the influence of small scale topographic features on large scale dynamics is even more pronounced than in the atmosphere. For the North Sea and Baltic Sea region the eye of the needle is the Danish Straits. For the ventilation of the Baltic Sea with salty and oxygen rich water from the North Sea the water has to pass through Little Belt, Great Belt or the Öresund. Under which circumstances inflow into the Baltic Sea occurs is conditioned by the history of the atmospheric circulation during the past months [*Matthäus and Schinke*, 1994] and dependent on local and instantaneous variations of sea level elevation around the Danish Straits [*Matthäus and Franck*, 1992].

The same general problem does reappear on the scale of regional climate models that also govern global climate models. Regional dynamics does determine global circulation like Denmark Strait overflow [*Käse et al.*, 2003] or Indonesian Throughflow [*Vranes et al.*, 2002] determine the heat transport in the Global Ocean. For regional climate models the range of scales to be considered has not reduced just because the resolution is higher. To resolve the

currents in the Baltic Sea would require a high horizontal and vertical resolution; probably of the order of 100 and 1m, respectively [*Omstedt and Axell*, 2003]. Even for spatially limited ocean models that cover North Sea and Baltic Sea only, a resolution of half a nautical mile or less is not yet feasible today for most research groups.

With the model setup comes also the decision to focus more on short term process studies and choose a higher resolution. Or the focus is on long term studies of regional climate and the need to parametrize the relevant processes. With the current setup of the coupled regional atmosphere-ice-ocean model RCA4-NEMO a compromise has been intended to allow for proper representation of the relevant processes that govern the atmospheric and oceanic circulation in the North Sea and Baltic Sea region. This is a requirement to long term simulations of a century or longer. Only then the coupled model system can be expected to respond to external forcing based on physical laws and not due to model artifacts.

In the current report the model setup of RCA4-NEMO is presented in section 2. With this setup CMIP3 [http://esg.llnl.gov:8080/] and CMIP5 [http://cmip-pcmdi.llnl.gov/cmip5/] scenarios have been downscaled from the middle of the last century till the end of this century. To build trust into the response of the RCM it needs to be validated against known, past conditions. Section 3 establishes one set of initial and boundary conditions for the RCM. As a first step of model evaluation an ERA40 hindcast with the coupled model is analyzed and discussed in section 4. The fields that establish the coupling between the model components are discussed and validated in section 5. The report finalizes with a summary and an outlook in section 6.

2 Model Description

2.1 Atmosphere Model

RCA is based on the numerical weather prediction model HIRLAM [*Unden et al.*, 2002] and is a primitive equation, hydrostatic model using a terrain-following hybrid vertical coordinate. In short, the RCA model is the climate version of the operational model HIRLAM. Since 1997, Rossby Centre has released four versions of RCA (RCA1, *Rummukainen et al.* [2001], RCA2 *Jones et al.* [2004], RCA3 *Samuelsson et al.* [2011]). The latest version is RCA4. Compared to the previous version RCA3, several new parameterizations have been introduced. The new lake model Flake is utilized in RCA4. Flake is a freshwater lake model capable of predicting the vertical temperature structure and mixing conditions in lakes of various depths on time scales from a few hours to many years [*Mironov*, 2008]. This scheme has been used in various numerical weather prediction (NWP) models, climate modeling, and other numerical prediction systems for environmental applications [*Martynov et al.*, 2010; *Mironov et al.*, 2010]. The *Kain and Fritsch* [1993] convection scheme has been updated to the Bechtold Kain-Fritsch scheme which separates the shallow and deep convection processes. A convection closure based on convective available potential energy (CAPE) [*Bechtold et al.*, 2001] is applied in RCA4 compared to RCA3, which might be more suitable for simulations with high-resolution. The soil hydrology in RCA4 is divided into a forest and an open land tile, respectively. The inclusion of soil carbon in RCA4 has reduced the overestimated soil-heat transfer in RCA3 and improved the simulated diurnal temperature range. *Pirazzini* [2009] found that the positive snow albedo-temperature feedback is an important factor in the high-latitude amplification of the global warming. The modifications in prognostic snow albedo have reduced the warm bias in cold climate conditions. For other physical parameterizations detailed description can be found in *Samuelsson et al.* [2011].

In this study, the RCA4 model domain has been set up on a 0.22°spherical, rotated latitude/longitude grid with 40 vertical levels. The model domain includes Europe, part of the North Atlantic, and the northern part of Africa (Fig. 1). Since the ocean plays an important role in the atmosphere-ocean interaction, the model domain covers the Northeast Atlantic, the Mediterranean Sea, the Black Sea and the North Sea and Baltic Sea. The North Sea and Baltic Sea are interactively coupled within RCA4-NEMO. For other ocean regions RCA4-NEMO uses prescribed ice- and ocean temperatures. Additionally ice albedo and the fractional ice cover is communicated to the atmosphere model, either prescribed from data or passed from the ice-ocean model.

2.2 Ocean Model

The ice-ocean component in the coupled system RCA4-NEMO is based on NEMO [*Madec*, 2011]. RCA4-NEMO uses the BaltiX setup [*Hordoir et al.*, 2013] for NEMO that covers the North Sea and Baltic Sea (Fig. 1). The BaltiX

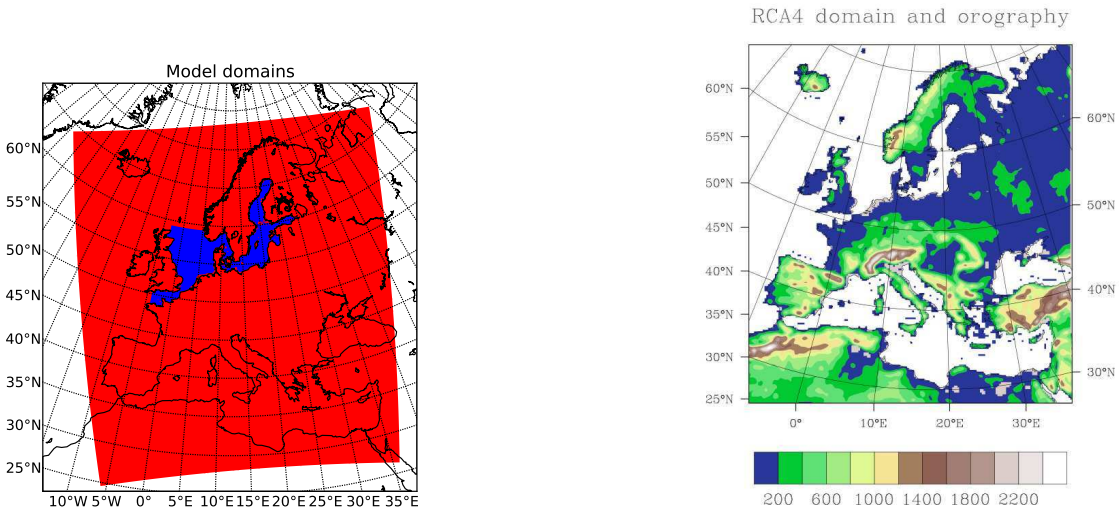

(a) *Model domains*

(b) *Orography*

Figure 1: Left) The model domains of RCA4 (red) and NEMO (blue); Right) The orography in RCA4 [m].

setup together with the NEMO engine constitutes a regional ocean model with open boundaries (cf. Section 3) across the northern North Sea and across the English Channel.

NEMO is a primitive equation model with a free surface. The BaltiX setup uses 56 geopotential levels as a discrete representation of the vertical coordinate with a minimum of three levels in shallow areas. The thickness of the levels increases from $3m$ near the surface to $22m$ in the Norwegian Trench. To allow for the large tidal range in the English Channel the geopotential coordinate surfaces are allowed to vary proportional to the free surface of the model [*Levier et al.*, 2007].

The horizontal resolution of the model is 2 nautical miles. That allows for mesoscale variability [*Meier et al.*, 2003] to be marginally resolved. Additional isopycnal background diffusivity and viscosity of $Ah = Am = 1m^2/s$ using a harmonic operator is applied to ensure numerical stability. Additionally, lateral mixing according to *Smagorinsky* [1963] was implemented into NEMO and is applied in the framework of the BaltiX setup [*Hordoir et al.*, 2013].

A $k-\epsilon$ turbulence model parametrizes the subgrid scale processes that lead to vertical mixing of momentum and tracers in the ocean. In the Danish Straits the resolution of the ocean model is not sufficient to resolve processes in the bottom boundary layer. To parametrize those processes a BBL submodel according to *Döscher and Beckmann* [2000] is used in BaltiX. The momentum dissipation on flat bottom is governed by a quadratic bottom drag and on lateral walls no-slip

conditions are imposed. The baroclinic time step of the ocean model is $6min$ with a barotropic subcycle of $6s$.

2.3 Ice Model

Within the NEMO framework the ocean model OPA is coupled to the sea ice model LIM3 [*Vancoppenolle et al.*, 2009]. LIM3 includes the representation of both the thermodynamic and dynamic processes. The ice dynamics are calculated according to external forcing from wind stress, ocean stress and sea-surface tilt and internal ice stresses using C-grid formulation from *Bouillon et al.* [2009]. The elastic viscous-plastic (EVP) formulation of *Hunke and Dukowicz* [1997] is used for the rheology. In the current setup for RCA4-NEMO LIM3 resolves five ice classes.

A comprehensive description of the ice model used in RCA4-NEMO is given in *Hordoir et al.* [2013].

2.4 Coupler

In the coupled model RCA4-NEMO the atmosphere and the ice-ocean component models interchange information about the processes at the air-sea and air-ice interfaces, respectively. The exchanged quantities are listed in Table 1 and a sketch is provided in Fig. 2. Basically, the ice-ocean component provides the information about temperature, albedo and the fractional ice cover. The atmosphere in turn does communicate the fluxes of heat, freshwater and momentum to the ice-ocean system.

Technically the coupling between the two model components is realized with the Ocean Atmosphere Sea Ice Soil Simulation Software (OASIS3) coupler, developed by the Project for Integrated Earth System Modeling (PRISM). This software allows synchronized exchanges of coupling information between numerical codes representing different components of the climate system [*Valcke*, 2006, 2012].

For the coupling process, OASIS3 acts as a separate mono-process executable, whose main function is to interpolate the coupling fields exchanged between the component models, and as a library linked to the component models and the PRISM model Interface Library (OASIS3 PSMILe). The Spherical Coordinate Remapping and Interpolation Package (SCRIP) [*Jones*, 1999] provided by Los Alamos National Laboratory is integrated in the OASIS3 coupler. SCRIP supports four re-mapping options: conservative remapping, bi-linear interpolation, bi-cubic interpolation and distance-weighted averaging, of which bi-linear and bi-cubic interpolations are suitable for logically rectangular grids. In this study, since the model domain only extends to mid-northern latitudes, and the grids of the atmosphere and ocean models are only slightly different, the bi-cubic method is used for the interpolations.

To communicate with OASIS3 directly, or with another model components, or to perform I/O actions, a component model needs to include a few specific PSMILe calls. OASIS3 PSMILe supports in particular parallel communication

Table 1: State variables and fluxes exchanges between the atmosphere and the ice-ocean model components in RCA4-NEMO. The arrows in the column coupler symbolize the bi-cubic interpolation from one grid to the other grid.

ice-ocean	coupler	atmosphere
sea surface temperature	$\longrightarrow$	
ice surface temperature	$\longrightarrow$	
ice albedo	$\longrightarrow$	
fractional ice cover	$\longrightarrow$	
	$\longleftarrow$	zonal wind stress over sea
	$\longleftarrow$	meridional wind stress over sea
	$\longleftarrow$	zonal wind stress over ice
	$\longleftarrow$	meridional wind stress over ice
	$\longleftarrow$	solar radiation over sea
	$\longleftarrow$	solar radiation over ice
	$\longleftarrow$	non-solar heat flux over sea
	$\longleftarrow$	non-solar heat flux over ice
	$\longleftarrow$	evaporation minus precipitation
	$\longleftarrow$	sea level pressure
	$\longleftarrow$	non-solar heat flux sensitivity

between a parallelized component model and the OASIS3 main process, based on the Message Passing Interface (MPI) and file I/O using the GFDL mpp_io library. All the necessary PSMILe calls have been implemented in the two models RCA4 and NEMO.

2.5 Model Performance

The experiments conducted so far have been using a domain decomposition for the atmosphere and for the ocean that tries to find a balance between resource usage and elapsed time. Increasing the number of nodes to divide the domains of the submodels into smaller subdomains does reduce the time it takes to calculate one model year. A large number of nodes on the other hand does increase the amount of communication between the nodes, because the information about the halo-rows around each subdomain must be sent to the neighboring nodes.

This issue is reflected in Fig. 3 where the elapsed time per model year levels out asymptotically with increasing number of cores. The elapsed time per model year does get shorter with increasing number of cores but the efficiency with which the resources are used is decreasing. So a domain decomposition was chosen for the models that uses a number of cores somewhere in the left part of the performance curve where it is steep. At the same time the allocation of nodes for each component model satisfied the condition that both the atmosphere and ocean model are elapsed for about the same time per model year.

Table 2 summarizes the elapsed time and the disk usage of an ERA40 run.

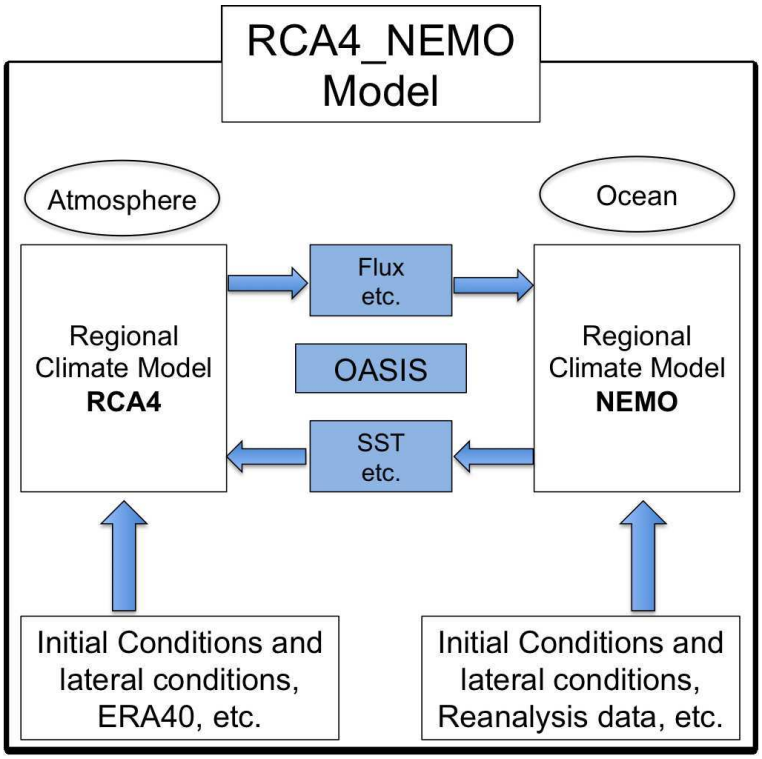

Figure 2: RCA4-NEMO work flow.

The measurements where taken on the Linux cluster Krypton [http://www.nsc.liu.se/systems/krypton/] which is running Intel E5-2660 processors. The averaged elapsed time per model year of about 9 hours does vary by plus minus half an hour with a 95% confidence level for an estimate of about 300 model years. The variance is mostly due to model years that had to be run with a somewhat shorter time step for the ocean model of five minutes instead of six minutes.

One year of model output that conforms to CORDEX [http://wcrp-cordex.ipsl.jussieu.fr/] and KLIWAS [http://kliwas.de/] specifications takes around 30GiB disk space. This includes monthly mean output for the ice-ocean model including all the prognostic variables plus diagnostic variables that are commonly analyzed. The output of the atmosphere model does include 6-hourly instantaneous values of the prognostic variables on selected pressure levels and surface values, 3-hourly values for radiation and cloud cover, 1-hourly wind at 10m, 1/4-hourly precipitation, daily output for the land surface model.

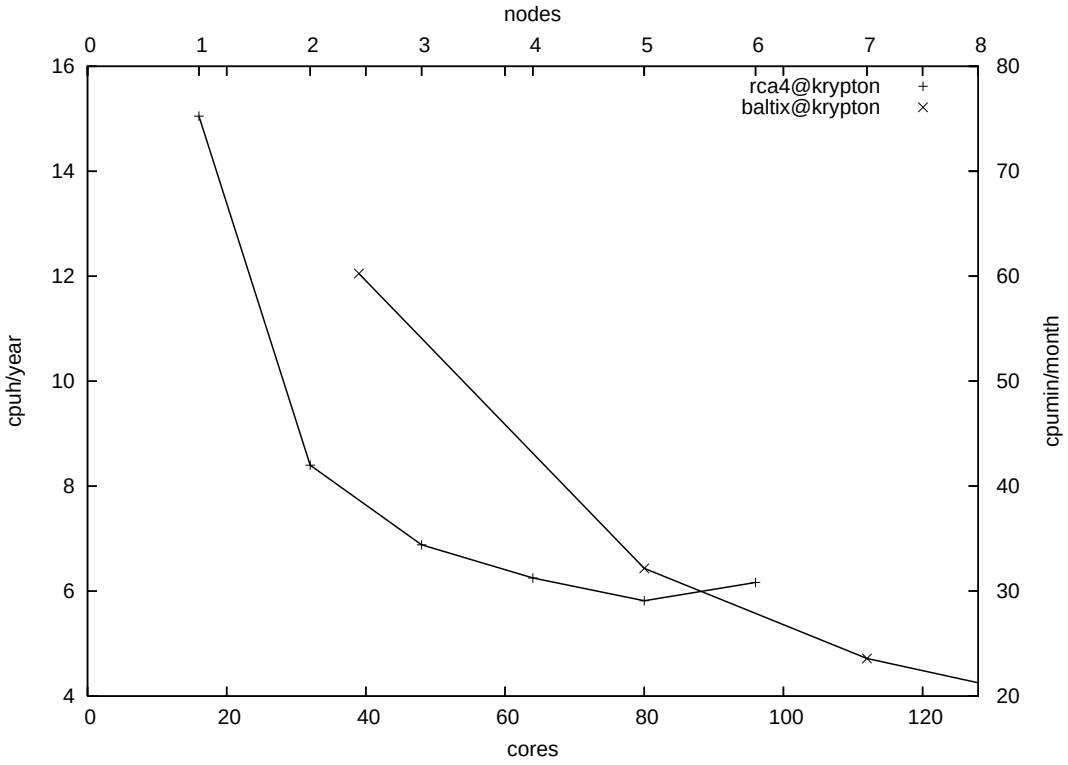

Figure 3: Elapsed time per model year with RCA4-NEMO for increasing number of nodes. The measurements have been taken on the Linux cluster Krypton (see text).

Table 2: Resource usage for the coupled model RCA4-NEMO on 10 nodes of the Linux cluster Krypton at the National Supercomputer Centre in Sweden (NSC).

	per model year	for 50 model years
cpu time	9 hours	19 days
model setup		1131 GiB
model input	11 GiB	550 GiB
model output	19 GiB	940 GiB

3 Initial and Boundary Conditions

3.1 Initial Conditions

The ocean model is started from rest. The Baltic Sea temperature and salinity are taken from a snapshot on 1 January 1970 of a reanalysis. The reanalysis is based on the Ensemble Optimal Interpolation approach and was applied to temperature and salinity for the Baltic Sea spanning the period January 1970 to December 1999. It has been carried out using the RCO model and the SHARK database [*Liu et al.*, 2013]. All temperature and salinity observations from the SHARK database have been used for this reanalysis. The root mean square deviations between reanalysis results and observations at all levels show that temperature and salinity have been improved significantly, compared to the simulation without data assimilation, by 31.1% and 38.8%, respectively. The vertical structure of the reanalyzed fields is also adjusted. Comparing the reanalysis fields and forecasting fields with independent CTD data, *Liu et al.* [2013] found significantly improved temperatures in middle and upper layers and for salinity even in deeper layers. Especially, the temporal variations of the deep water salinity caused by saltwater inflows are improved. Moreover, the reanalysis has improved the depth of the halocline and thermocline (compared to observations) which are overestimated in the run without data assimilation.

The reanalysis fields for 1 January 1970 were used for the initialization of the model Baltic Sea on 1 January 1961. That is reasonable since the state of the Baltic Sea was relatively stable during this period. With an initial temperature and salinity distribution the spin-up time is reduced considerably even if the chosen year of the reanalysis does not match the starting year of the ice-ocean model.

In the North Sea the initial temperature and salinity distribution is a bi-linear interpolation onto the model grid from the climatological January mean of the climatology by *Janssen et al.* [1999]. The climatology is an average over the conditions during the last century, biased towards the end of the period, where more data is available. Since the North Sea does not have a long memory of past conditions the initial conditions for the North Sea was deemed much less critical, than the one for the Baltic Sea.

The initial fields for the atmosphere and for the land surface model are interpolated from the ERA40 data-set.

The ice model starts with no ice at all, since the Baltic Sea does not produce multi-year ice.

3.2 Open Boundary Conditions

Processes in the adjacent Northeast Atlantic have a profound impact on the circulation and hydrography of the North Sea. Within the concept of a regional model the impact of the region outside the model domain must be taken into account by some sort of boundary conditions. Since the boundary of the model domain does not constitute a physical boundary the formulation of proper con-

ditions on the differential, and for the numerical model the difference, equations is difficult.

A traditional approach by *Orlanski* [1976] aims to radiate wavelike motions from the model domain without reflection on the open boundary. Basically that comes down to calculate the phase speeds in the model domain and extrapolate those to the boundary of the model domain where calculations including gradients normal to the open boundary cannot be applied due to the lack of information on the other side of the boundary. That applies to barotropic motion from within the model domain.

To allow volume transport to take place across the open boundary the barotropic transports are prescribed [*Hordoir et al.*, 2013].

Since the regional ocean model does not take into account a tidal potential the tides in the model domain are Kelvin waves that need to be prescribed on the open boundary. In the current setup 11 tidal components are used from the global tidal model at the Oregon State University [http://volkov.oce.orst.edu/tides/] [*Egbert and Erofeeva*, 2002]. The tidal components are those deemed relevant for the North Sea, namely M2, S2, N2, K2, K1, O1, P1, Q1, M4, MS4, MN4. For a validation of the tides in the regional model see *Hordoir et al.* [2013].

The baroclinic circulation at the open boundary is left for the model to be calculated from the geostrophic wind. On average this yields a northward baroclinic current along the Norwegian coast and a southward current offshore. Also in the Feie-Shetland section and the Fair-Isle Current of the density structure yields inflow from the Atlantic. During conditions of inflow temperature and salinity are prescribed from external sources. For the experiments discussed in this report climatological seasonal cycles for T and S as compiled by *Levitus et al.* [1994]; *Levitus and Boyer* [1994] have been used. That does rule out the telecommunication of signals through oceanic processes from the Atlantic into the North Sea. It is well known [*Becker and Pauly*, 1996] that the North Sea answers to varying NAO indices not just through atmospheric forcing. In the scenarios simulations conducted with this model setup temporally resolved temperature and salinity fields from the global ocean models are prescribed at the open boundaries to allow the regional model to respond to changes in the global ocean through advection of signals in the ocean.

The boundary data for the atmosphere is ERA40 data [*Uppala et al.*, 2005]. The atmospheric boundary data is the main forcing for the presented simulations. Since reanalysis data is supposed to mimic the evaluation of the real weather, model results can be directly compared to observations.

3.3 River Runoff

River discharge is the crucial part in the water balance of the North Sea and Baltic Sea and therefore a very important boundary condition. Especially for the Baltic Sea – which is generally speaking an outflow regime – the amount of river discharge defines the state substantially.

The river discharge used in the simulations described in this report is based on E-HYPE [*Lindström et al.*, 2010] results. The input data for E-HYPE was

taken from an RCA3 simulation forced with ERA-interim at the boundary. The used river discharge reflects natural fluctuations as the seasonal cycle and year-to-year variability (Fig 4+5). According to the period of ERA-interim the data covers the years 1979–2008. For the period 1961–1978 a monthly climatology of the period 1979–2008 was used.

In the following area and decadal mean discharge is compared to the river discharge as used previously [*Hordoir et al.*, 2013]. Here, the numbers are based on observations. For more information on the origination of this data the reader is referred to *Meier* [2007] for the Baltic Sea and the UK Met Office (*personal communication, 2012*) for the North Sea. It should be noted that the former river discharge for the North Sea was monthly climatology only.

Table 3: Climatological river discharge $[m^3/s]$ in the entire model domain and separated for basins (cf. Fig 6) as computed with E-HYPE and as used previously.

	E-HYPE	based on observations
total	28457	27034
North Sea and Skagerrak	12592	12704
Baltic Sea	15371	14152
Danish Straits	493	179

As shown in Table 3, the time averaged river discharge is in general agreement between E-HYPE results and formerly used runoff based on observations (referred to as observations). The total discharge in the model domain adds up to $28457 m^3/s$ and $27034 m^3/s$ for E-HYPE and observations, respectively. The slight overestimation appears mainly in the Baltic Sea area whereas the amount of fresh water is very similar in the North Sea (Table 3).

Table 4: Long-term means (9 year chunks) of river discharge $[m^3/s]$ from all rivers east of 13.07°E as computed with E-HYPE and as used earlier e.g. by *Meier* [2007] (based on observations), respectively.

decade	E-HYPE	observations	difference
1961-1969	15371	14117	+8.88%
1970-1978	15371	13180	+16.62%
1979-1987	16173	15275	+5.87%
1988-1996	15104	14773	+2.24%
1997-2005	15040	14171	+6.13%

However, using a climatological discharge for the period 1961–1978 introduces some inaccuracy. The monthly climatology misses the year-to-year variability (Fig. 5). This leads to a considerable overestimation of the runoff since the period was drier than on average according to the observations. In particu-

lar for the period 1970–1978 the discharge in the climatology is more than 16% larger than observed for the Baltic Sea area (Table 4). This makes the Baltic Sea fresher and obstructs inflows from the North Sea.

The seasonal cycle of river runoff is well represented in the E-HYPE forcing data (Fig. 4). The highest discharge into the Baltic Sea occurs during April and May as a consequence of the snowmelt. That is in agreement with observations whereas the seasonal peak is more pronounced in observations.

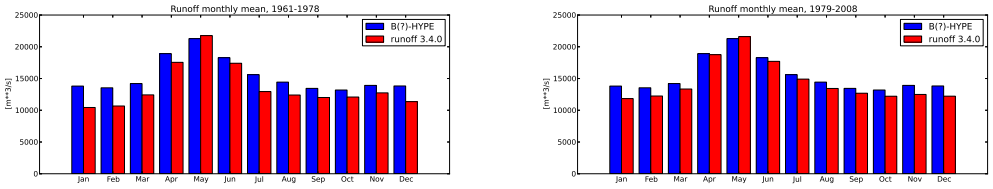

Figure 4: Climatological river discharge for the Baltic Sea region.

The matching of the year-to-year variability with observations can be seen in Fig. 5. The correlation of monthly series is 0.830 between 1979 and 2008. However, the standard deviation is somewhat larger in the observations ($4050 m^3/s$) than in the E-HYPE data ($3290 m^3/s$).

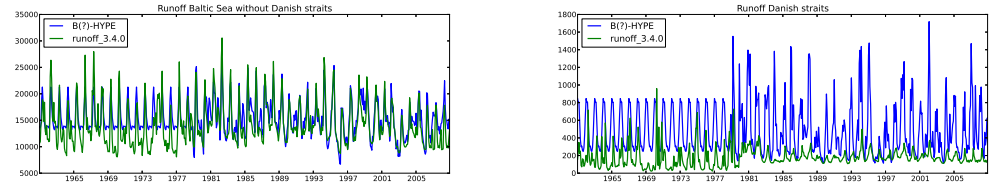

Figure 5: River runoff for the Baltic Sea (left) and the Danish Straits region (right) as indicated in Fig.6.

Finally, it should be mentioned that the number of river mouths increased significantly from the processed observational data to the E-HYPE data set (Fig. 6). Whereas the river runoff was discharged into the Baltic Sea at 29 locations in the former forcing [*Meier*, 2007] the number increased to almost 300 in the E-HYPE runoff data set applied.

Looking into smaller regions like the area of the Danish Straits (see blue box in Fig. 6) the differences can be even more pronounced. Whereas there are plenty of river mouths in the E-HYPE data there is only a single discharge location in the former set. The consequence is a mean discharge of $493 m^3/s$ (E-HYPE) and $179 m^3/s$ (formerly), respectively. Herewith, the fresh water supply is almost three times larger in the new forcing data set. Effects on model results can be considerable especially since the differences appear in a region crucial for water and salt exchange between the North Sea and Baltic Sea.

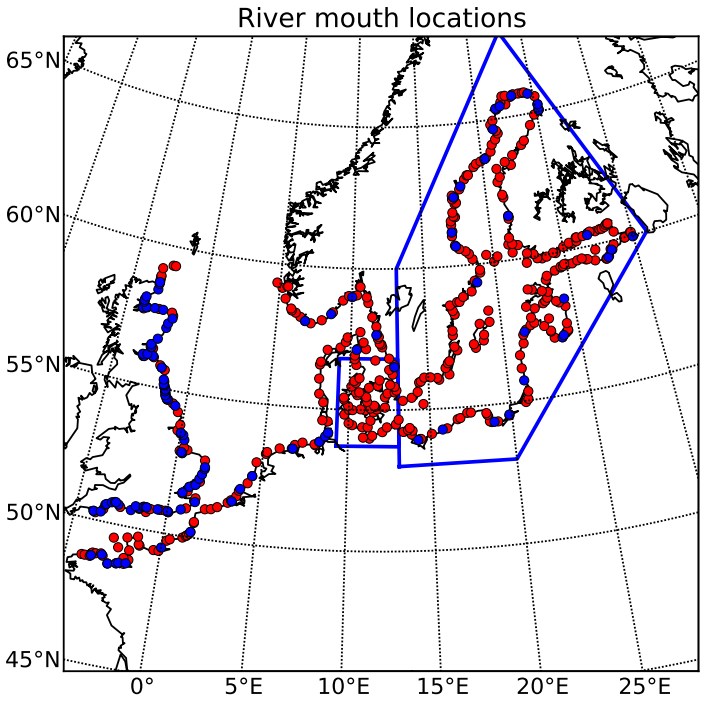

Figure 6: River mouth locations. Blue: River mouth locations in the processed observational data set. The polygons highlight the Baltic Sea and Danish straits river discharge discussed in Fig. 5+4.

4 Validation of an ERA40 Simulation

4.1 Ocean

4.1.1 Circulation

The circulation of the shallow Baltic Sea is wind-driven and cyclonic as shown in earlier studies [e.g. *Krauss and Brügge*, 1991; *Lehmann et al.*, 2002; *Meier*, 2007]. A simplified circulation model for the Baltic was also proposed in *BACC* [2008]. Some features of the circulation in the Baltic Sea are properly captured by RCA4-NEMO (Fig.7).

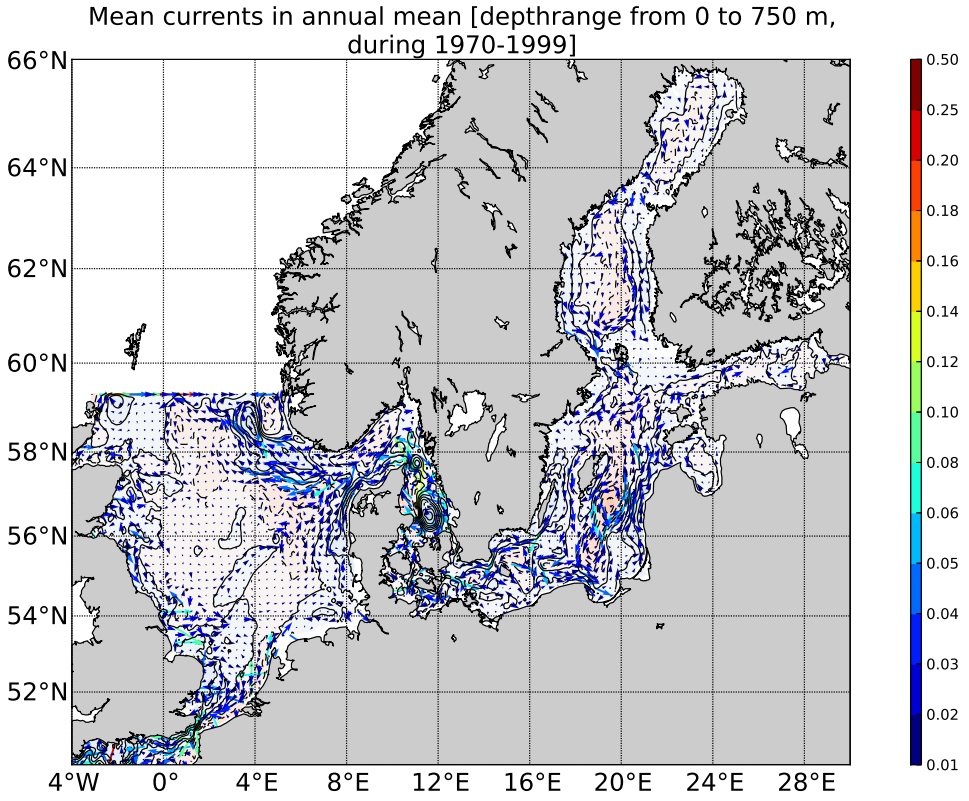

Figure 7: Mean vertically integrated circulation during 1970-1999 in RCA4-NEMO. The magnitude of the current vectors is shown with different colors in units ms^{-1}, whereas the contours represent corresponding stream function.

The inflowing waters from the North Sea to the Baltic Sea follow the deep channels connecting different basins of the Baltic Sea, whereas the freshwater

leaves the Baltic in the surface layers. The main outflow path from the central Baltic to the Arkona Basin is along the Swedish coast in the Western Gotland Basin. The inflow from the Arkona Basin appears to the south of the outflow and is directed to the center of the Bornholm Basin. The inflow to the inner parts of Baltic Sea continues through the Stolpe Channel along the eastern side of the Gotland Basin, whereas some of water flows through the Gdansk Basin ventilating the southernmost area of the Baltic Sea.

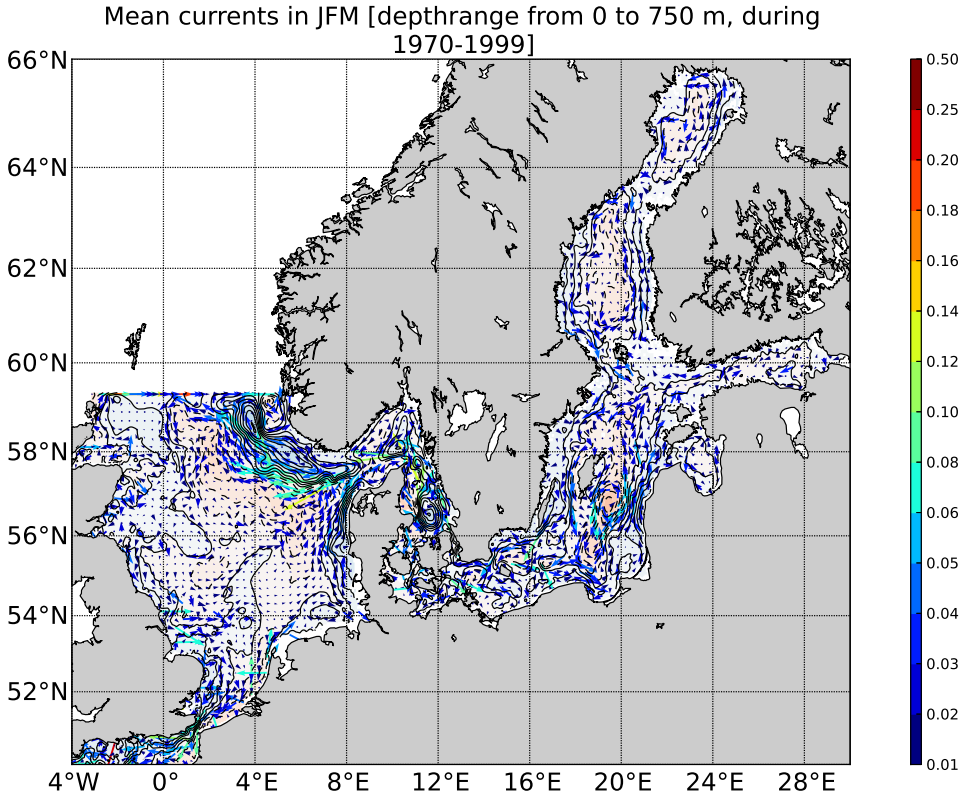

Figure 8: Mean vertically integrated circulation during 1970-1999 for the winter season in RCA4-NEMO. The magnitude of the current vectors is shown with different colors in units ms^{-1}, whereas the contours represent corresponding stream function.

The general circulation in the terminal basins of the Baltic is also cyclonic[e.g. *Alenius et al.*, 1998; *Andrejev et al.*, 2004; *Myrberg and Andrejev*, 2006] but with dominating mesoscale features (eddies, jets, etc). In the Gulf of Finland, the inflow appears along the southern and outflow along the northern coast. The

effect of large freshwater input to the Gulf of Finland and Bothnian regions is visible as large outflows from the basins.

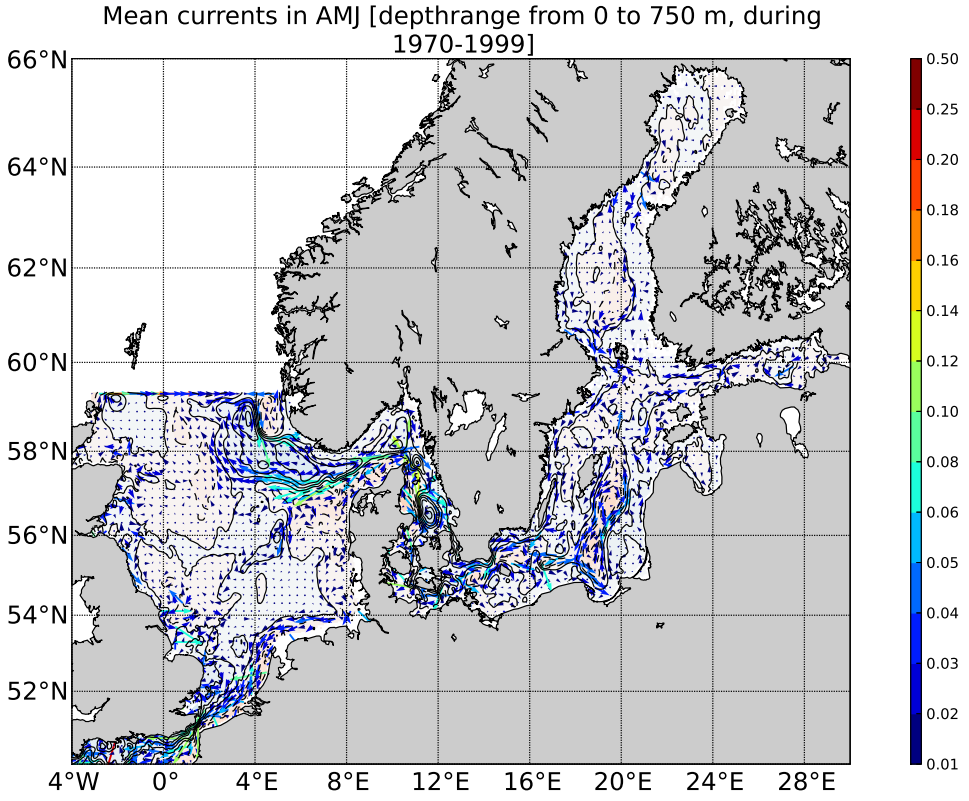

Figure 9: Same as Fig. 8 for spring.

The seasonal cycle of the circulation strength is substantial due to seasonal changes in the wind patterns, but the circulation patterns prevail. Namely, the mean barotropic currents in the Baltic are strongest during winter (JFM) and autumn (OND), while the weakest values occur during spring (AMJ) and summer (JAS), but the cyclonic circulation with inflowing/outflowing paths is visible in all seasons (Fig. 8-11).

The circulation of the relatively shallow North Sea is also cyclonic and wind-driven due to dominating westerly winds [e.g. *Sündermann and Pohlmann*, 2011; *Winther and Johannessen*, 2006]. Under westerly winds relatively strong southward currents dominate along the British coast, whereas northward currents dominate along the Danish coast. The outflow from the Baltic is visible as the Norwegian Coastal Current along the Norwegian coast.

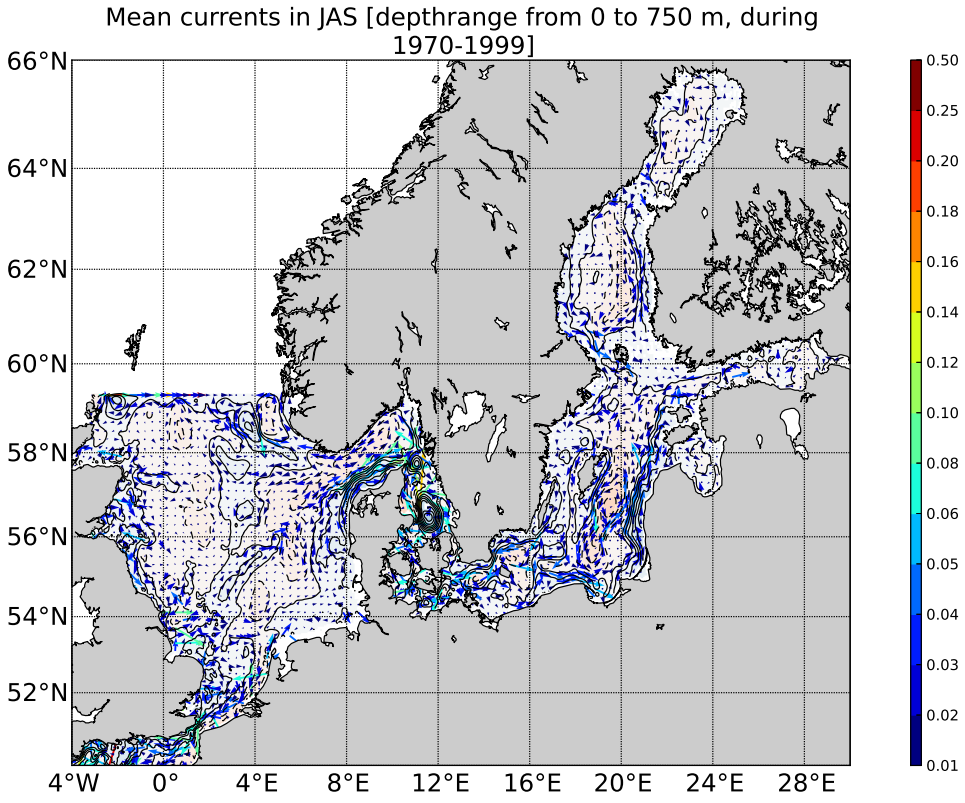

Figure 10: Same as Fig. 8 for summer.

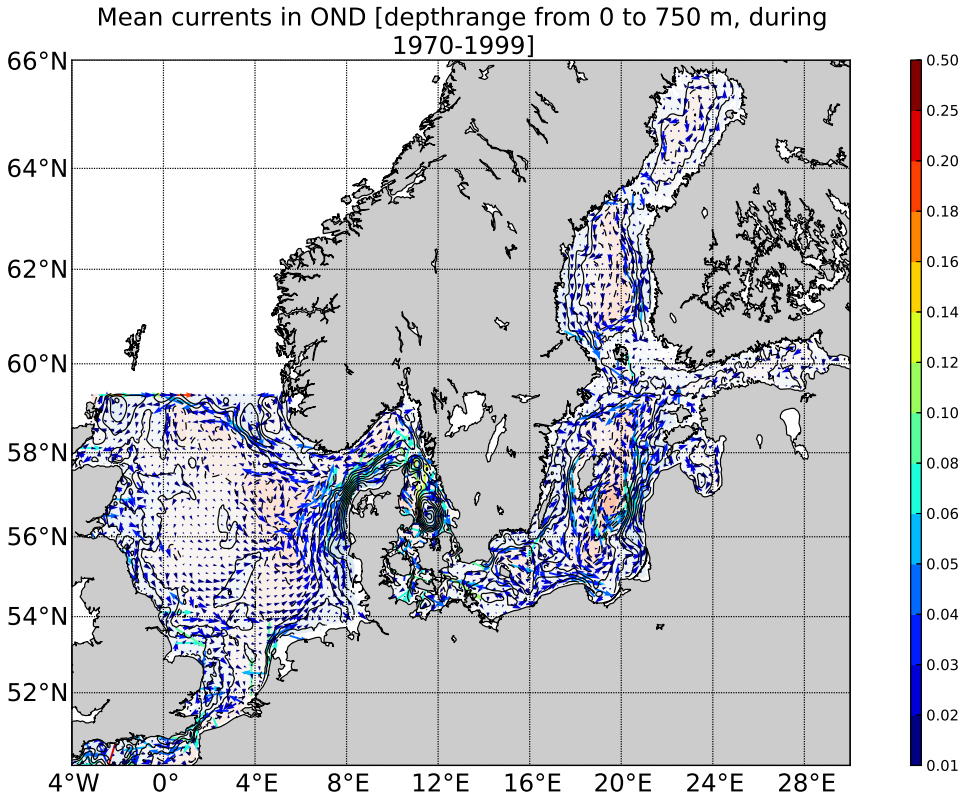

Figure 11: Same as Fig. 8 for autumn.

The seasonal cycle of the circulation patterns appear to be quite strong in RCA4-NEMO. The strongest cyclonic circulation is seen during autumn (OND) and winter months (JFM) and is somewhat weaker or reversed in summer (JAS) and spring (AMJ). The reversal is seen as a strong southward current along the Dutch and Belgium coasts and an outflow through the English Channel.

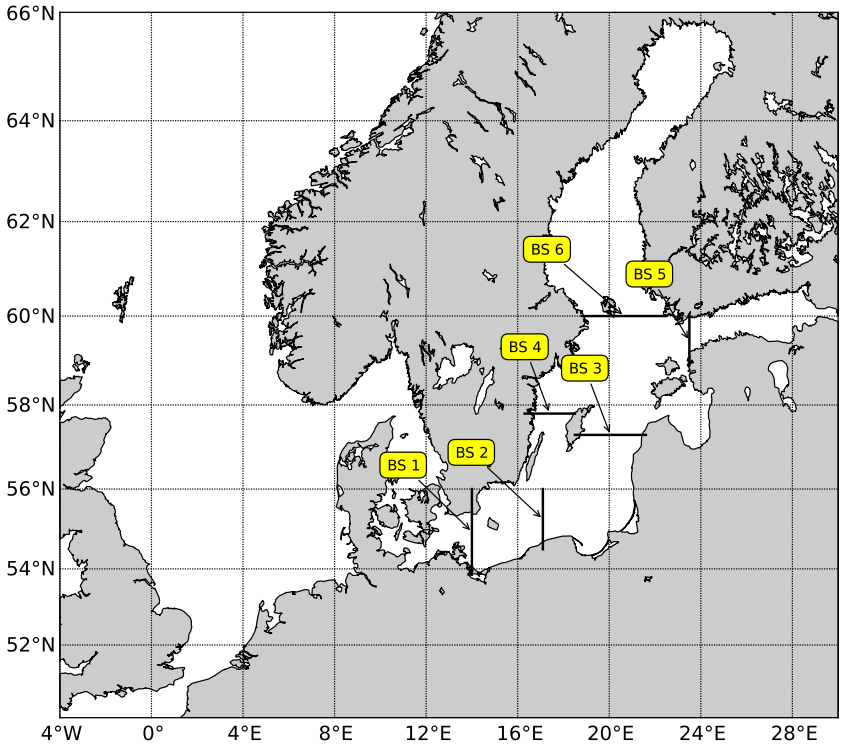

Figure 12: Transects used for calculating the volume transport in the RCA4-NEMO.

The volume transports through different sections in the Baltic Sea are shown in Table 5 and compared with the values obtained with other three-dimensional ocean models for the Baltic Sea. The Rossby Centre Ocean Model (RCO) has been used in numerous studies and been validated extensively during previous years. More information about the RCO can be found in *Döscher et al.* [2002]; *Meier* [2007] and from references therein.

The outflow from the Baltic through Arkona Basin is slightly lower in RCA4-NEMO than in RCO or values obtained by *Lehmann and Hinrichsen* [2002],

Table 5: Mean volume transports $[10^4 m^3/s]$ for different sections in the Baltic Sea during 1971-1999 (cf. Fig 12) calculated from RCA4-NEMO and Rossby Centre Ocean model (RCO)

Transect	RCA4-NEMO	RCO	Literature
BS 1	-1.47	-1.68	-1.6 [*Lehmann and Hinrichsen*, 2002]
BS 2	2.17	3.89	6.89 [*Lehmann and Hinrichsen*, 2002]
BS 3	5.28	7.08	no data
BS 4	-6.46	-8.15	no data
BS 5	-0.37	-0.36	-0.36 [*Andrejev et al.*, 2004]
BS 6	-0.47	-0.41	-0.54 [*Myrberg and Andrejev*, 2006]

whereas the values for the Baltic Proper circulation differ more substantially. The inflowing volume transport through Stolpe Channel to the eastern Baltic Proper in RCA4-NEMO was lower than reported by *Lehmann and Hinrichsen* [2002] or in RCO. The large discrepancy between the *Lehmann and Hinrichsen* [2002] and RCO is due to difference in the location of the selected transect, but nevertheless in RCA4-NEMO the value seems too low. The low volume transport through Stolpe Channel affects the bottom salinity of the Baltic Sea - the salinity is underestimated at 200 m depth in BY15 in RCA4-NEMO (cf. Appendix, Fig. 52).

The cyclonic circulation of the Baltic Sea is also affected by lower inflow through Stolpe Channel. The inflow through BS3 (transect between Gotland and Latvia) and outflow through BS4 (transect between Swedish mainland and Gotland) are lower than the corresponding values from RCO. The outflow from the Gulf of Finland is in agreement with the values obtained by RCO and *Andrejev et al.* [2004], whereas the outflow from Bothnia is slightly larger than in RCO.

4.1.2 Hydrography

Baltic Sea

The deep water salinity in the Kattegat matches the observations fair enough while the salinity towards the surface is underestimated by several psu (see Appendix Fig. 37-40). This is a clear indication for a too strong freshwater export from the Baltic Sea. Moving further into the Baltic Sea the near bottom water becomes too fresh, too. For instance at BY2 – a station located at eastern edge of the Arkona Basin – the bottom salinity is almost 4 psu too low. This underestimation penetrates then further into the Baltic Sea where the near bottom salinity is generally underestimated (see Fig. 13 for BY15). Obviously, there is not enough salt entering the Baltic Sea or in other words the number and/or size of inflows is not properly represented in the model. Please keep in mind that the mean river discharge is somewhat overestimated but in general agreement with observations. Consequently, this can be only part of the problem. An-

other issue is the too shallow mixed layer in the Baltic Sea. Beside the upward shifted pycnocline gradients are not as strong as in observations. Examinations on this topic are ongoing in the moment and will hopefully improve results in the future.

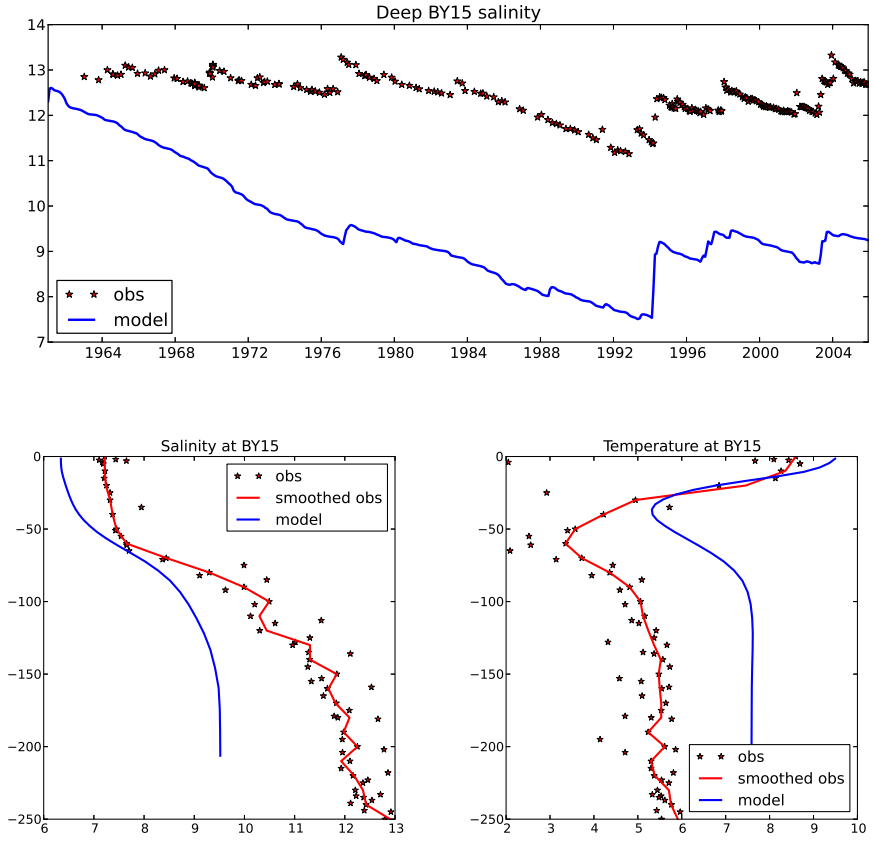

Figure 13: BY15

The salinity time series (Fig. 49-52) reveal that beside the general underestimation of surface salinity, its variability is often strongly underrepresented. For instance at Landskrona where the simulation ranges from 7–17 psu and the observations from 7–27 psu. Regarding the bottom salinity, all modeled Baltic Sea stations show a clear reduction at the beginning of the simulation until a new stable equilibrium is reached after a couple of years. After the initial years, most major inflow events seem to be realistically reproduced by the model in terms of the salinity jump connected with it (e.g. Fig. 13). However, in the general fresher water it is also easier for salt water inflows to penetrate deeper into the Baltic Sea.

The temperature profiles (Fig. 41–44) match the observations satisfyingly in the Kattegat more or less at all depths. However, for stations in the Baltic Sea the deep water is generally too warm by a couple of degrees (see Fig. 13 for BY15). In terms of variability of near bottom temperature, no general conclusion can be made. While at some places (mainly in the Kattegat and the entrance of the Baltic Sea) the variability is extremely underestimated compared to observations (basically, there is no variability in the model) other places have quite some variability where observations show only little (e.g. in the central Baltic Sea [BY15 and BY38]).

North Sea

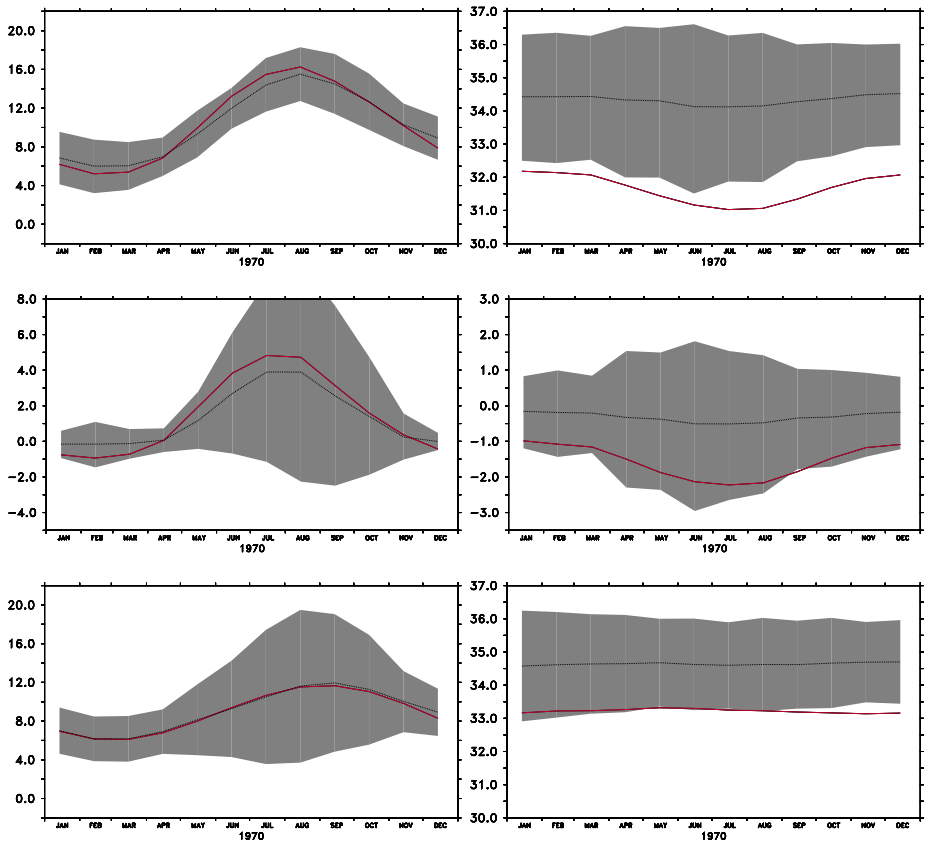

Figure 14: Climatological (1970 - 1999) sea surface values (top row), vertical range (middle row) and near-bed values (bottom row). The black curves represent the *Berx and Hughes* [2009] climatology. The gray shading indicates the 95% confidence interval, assuming Gaussian distributions. Temperatures [°C] are depicted in the left column and salinities [psu] in the right one.

The evaluation of North Sea temperatures and salinities from the ERA40 hindcast experiment with RCA4-NEMO is based on a comparison with climatologies and with timeseries from the MARNET [http://www.bsh.de/de/Meeresdaten/Beobachtungen/MARNET-Messnetz/] database. First the discussion concentrates on common features and differences between the climatological record of *Berx and Hughes* [2009] and the model variables.

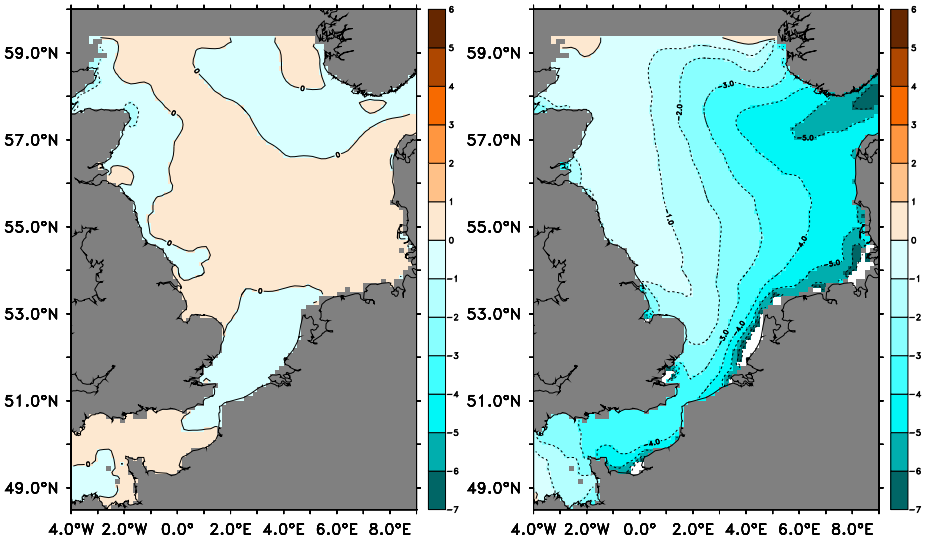

Figure 15: Climatological (1970 - 1999) annual mean sea surface biases. The biases represent the model-data differences relative to the *Berx and Hughes* [2009] climatology. Temperatures [°C] are depicted in the left column and salinities [psu] in the right one.

The ICES [http://www.ices.dk/] climatology provides sea surface temperatures and salinities and near-bed temperatures and salinities across the European Shelf. A distinct advantage of the climatology by *Berx and Hughes* [2009] is the averaging period of 1970 - 1999 which matches the climatological period defined for RCA4-NEMO.

In Fig. 14 a general agreement between observations and model results can be established for sea surface and near-bed temperatures. More than 95% of the model realizations lie within the range of the estimated true values. For salinities in Fig. 14 this is not the case. There is a large export of freshwater from the Baltic Sea that does spread across the North Sea during the course of the experiment. But the Baltic Sea is not the sole source of too much freshwater (see the MARNET timeseries for salinities below).

On annual mean maps for the model biases of temperature (Fig. 15-17) an overall agreement between the model result and the observations is evident. Generally surface temperatures do not deviate more than ± 1°C from

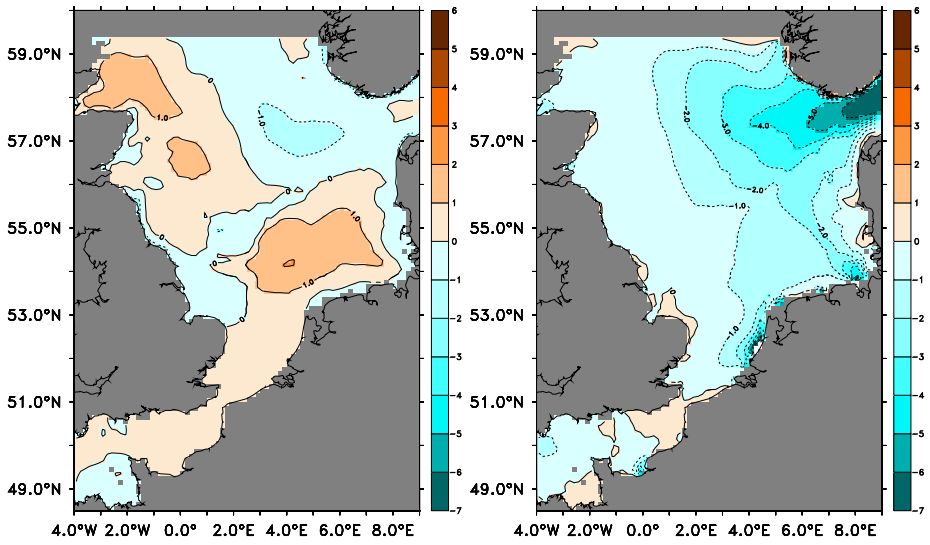

Figure 16: Same as Fig. 15 for the mean vertical range biases.

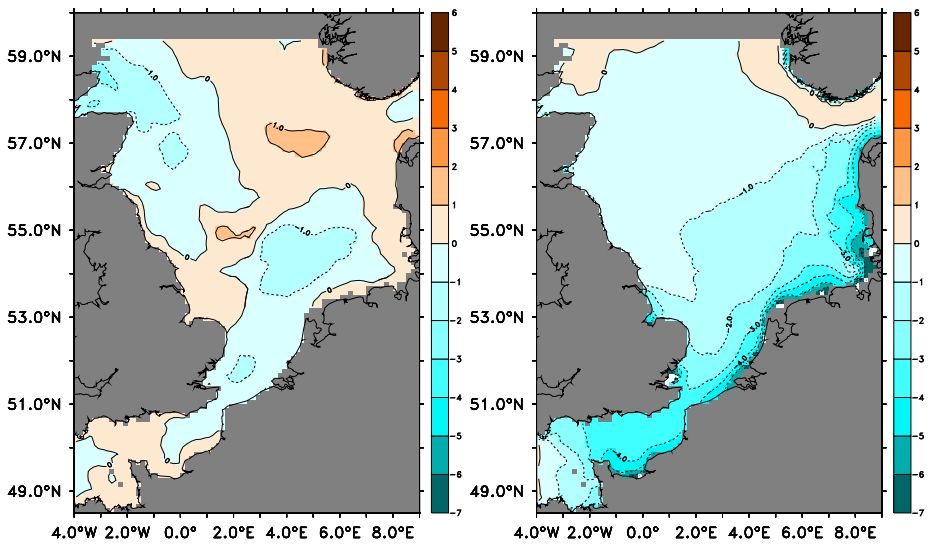

Figure 17: Same as Fig. 15 for the mean near-bed biases.

the *Berx and Hughes* [2009] climatology. Bottom temperatures and the vertical temperature range are with ± 2°C of the ICES climatology.

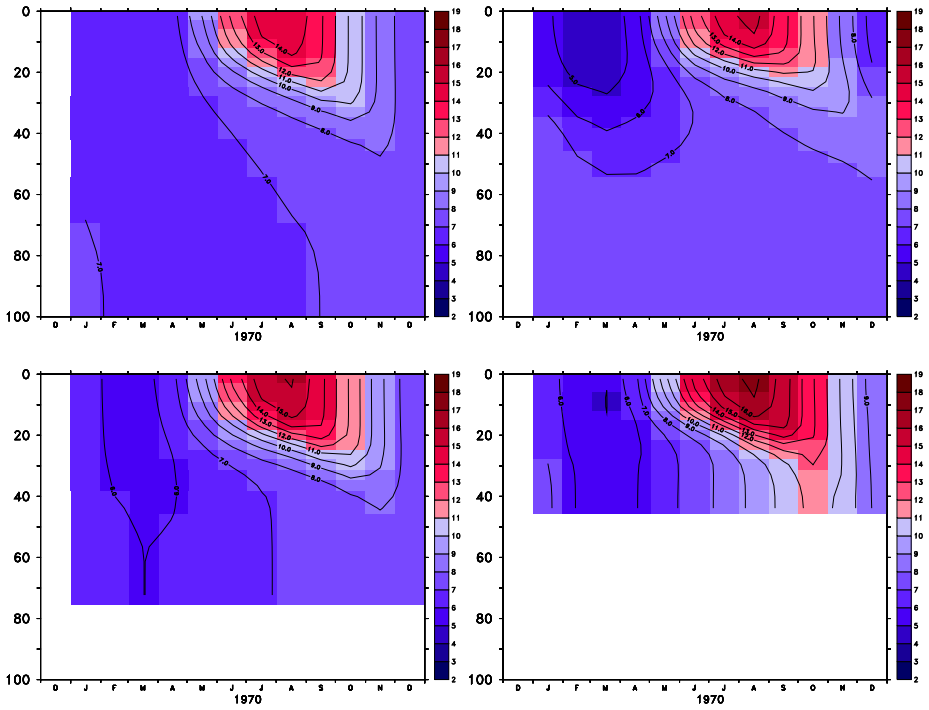

Figure 18: Hovmüller diagram of climatological seasonal cycles of temperatures at selected positions across the North Sea. Locations: 0°E, 58°N (top left), 5°E, 58°N (top right), 1°E, 56°N (bottom left), 5°E, 54.5°N (bottom right).

For salinity the biases (Fig. 15-17) are far too large to be realistic. The model realization suffers from freshening of the North Sea by several sources. The reasons are not yet understood. However a number of plausible causes are identified and for the next version of RCA4-NEMO we strive to eliminate this issue [see section Outlook (6)].

Figure 18 illustrates the climatological seasonal cycle of simulated temperatures in the water column at selected locations. At 58°N the summer warming of the water column does not reach as deep as has been recorded for the period 1902-1954 in *Tomczak and Goedecke* [1964]; *Goedecke et al.* [1967]. This might indicate that the vertical mixing in this region of the model domain is not as strong during summer as it should be. During winter the model is generally too cold and the winter water does persist until late in summer at relatively shallow depths. The overall structure of the isotherms loosely matches climatological records. At the two positions at 58°N the surface water is below 7°C during winter and rapidly warms in May to reach 14°C during Juli and August.

The two stations further south where the effects of the tides on the stratifica-

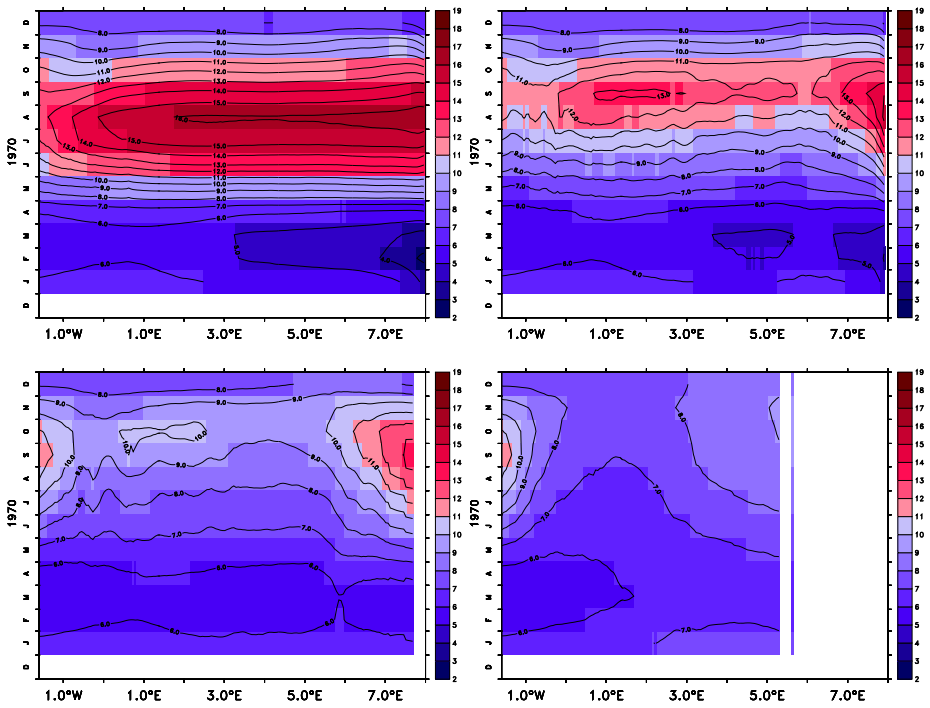

Figure 19: Hovmüller diagram of climatological temperatures in selected depth horizons across the North Sea at 56.5°N. Depths: 5m (top left), 20m (top right), 30m (bottom left) and 50m (bottom right).

tion are more pronounced the isotherms during the climatological year compare better with climatological records (bottom row of Fig. 18). At 56°N the water column is still too cold by 1°C during the coldest months and the seasonal thermocline is too shallow by around 10 m. At the station in the German Bight the model simulation misses the subsurface maximum during late summer. In the model the warmest temperatures are found right at the surface. Thought the modeled temperatures at the station at 54.5°N show clear signs of vertically homogenization the stratification during summer remains too strong.

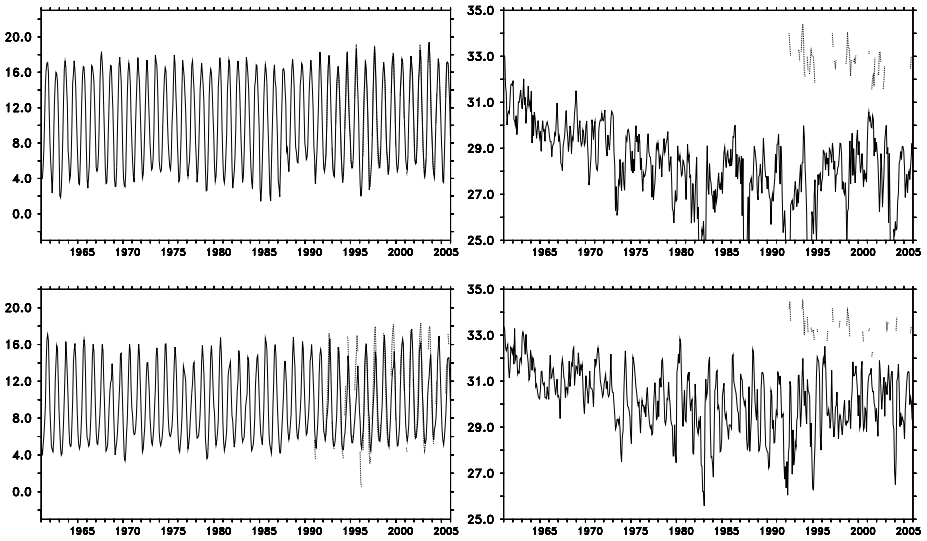

Figure 20: Temperature [°C] (left) and Salinity [psu] (right) timeseries at the lightship station Deutsche Bucht (07.45°E, 54.17°N) in 8m (top row) and 30m (bottom row). The dashed curve is the record from the MARNET database and the solid curve is from the model simulation.

The temperature distribution in specific depth horizons (Fig 19) allows for an inspection of the seasonal cycle with varying longitude. In all depth horizons the amplitude of the seasonal cycle of temperature is stronger in the eastern North Sea. At the latitude of 56.5°N it amounts to 10°C between March and September. In the western North Sea the seasonal cycle is weaker with a temperature difference of around 6°C. Near the surface summer temperatures are too high across the North Sea. In October a rapid cooling can be inferred from Fig 19 which might be due to a shallow mixed layer as discussed in the previous paragraph. In winter the temperatures are somewhat too low. At intermediate depths the region north of the Dogger Bank shows a maximum in summer temperatures and a minimum in winter temperatures which is in agreement with climatologies. At the Danish coast the temperatures in 20m and 30m seem to be influenced by non-local effects. Either by downward heat transport through the water column or by a transport of warmer water from the south by the currents

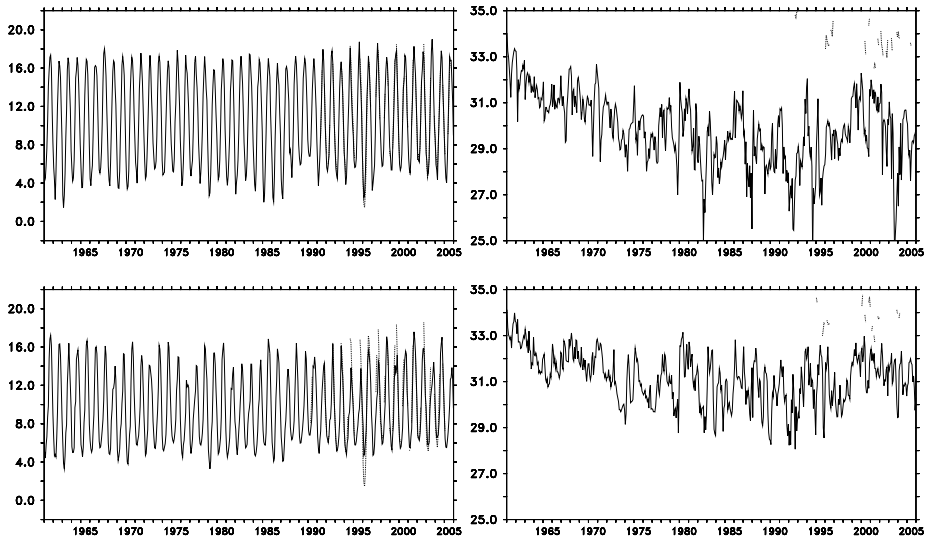

Figure 21: Same as Fig. 20 but for the lightship station Ems (06.35°E, 54.17°N).

along the Danish coast. This can give helpful clues to identify shortcomings in the model setup.

A comparison with the MARNET database maintained by the German Federal Maritime and Hydrographic Agency (BSH) reveals that during the spin-up phase of RCA4-NEMO up to 4 psu of salt is lost in the German Bight. Figures 20+21 compare records of temperature and salinity at lightships Deutsche Bucht and Ems with those from the model simulation. Temperature is in reasonable agreement although the winter temperatures are too cold and the summer temperatures too warm. This is specially true for the deep record at 30m depth.

4.1.3 Ice

The model is able to reproduce the ice conditions in the Baltic Sea reasonably well during the simulation period (Fig. 22 and Fig. 23). The sea ice extent during 1970-1999 is slightly underestimated, but the variability is captured reasonably well. The correlation between the simulated and observed ice extent area is more than 0.96 with the mean difference of 15.2 km^2 and root mean square difference of 30.6 km^2 between the series.

Mean ice cover during February averaged over 1963-1979 is comparable with the climatological observed values for late February. The observed values are taken from the climatological ice atlas [*Udin et al.*, 1982] for 21 February, whereas the model results are temporal means over the whole month. The climatological mean ice concentration in the model is underestimated, but the main features of the Baltic Sea ice cover are well represented.

The largest concentrations appear in the northern- and easternmost areas

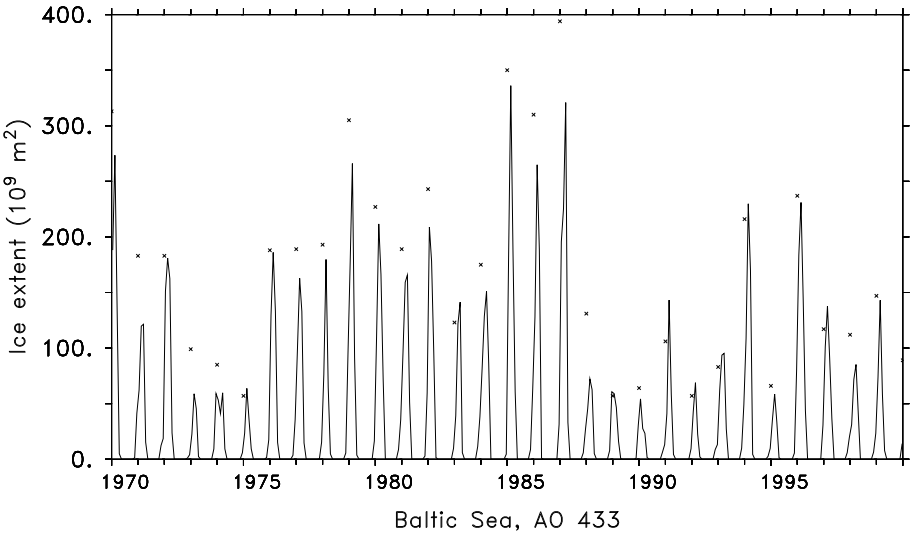

Figure 22: The simulated Baltic Sea ice extent from monthly mean ice concentration larger than 0.02 (black line) with the observed maximum ice extent (black crosses).

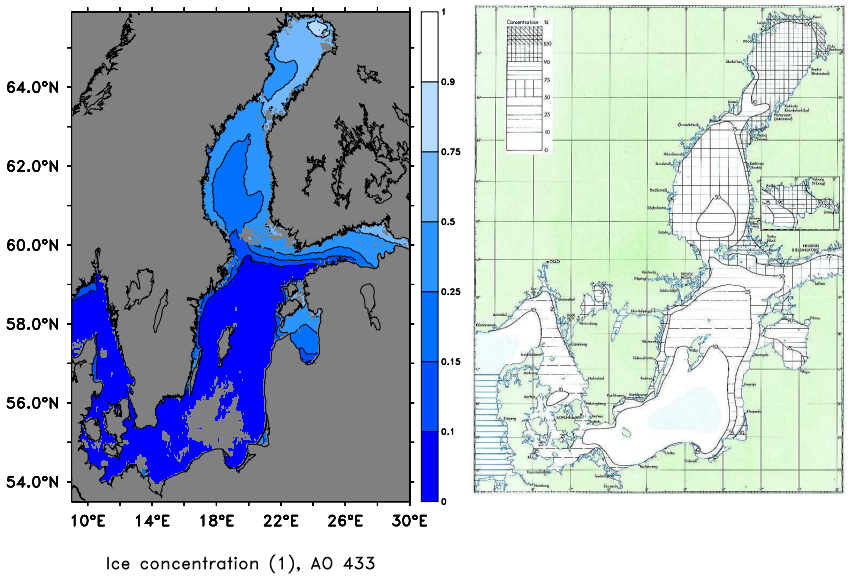

Figure 23: The mean Baltic Sea ice concentration in February from the model (left) and in 21 February from observations from *Udin et al.* [1982](right) during 1963-1976.

of the Baltic Sea - the Bothnian Bay and Gulf of Finland. In the other parts of the Baltic Sea the ice concentration is lower. Lowest mean values appear in the largest basin of the Baltic Sea - the Baltic Proper. The location of the concentration more than 0.25 is placed further in the north in the model compared to the observed values, but the large discrepancy might be due to the averaging of the model results. In the early February, the Baltic Sea ice coverage is not yet formed, the maxima occurs somewhere in the late February/early March dependent on the severeness of the winter.

4.2 Atmosphere

This section gives a brief comparison of measured and modeled 10m-wind speed. That is done for RCA4-NEMO as well as RCA4 standalone. As shown below, differences between the coupled and the uncoupled simulation are rather tiny since they are related to differences in the modeled and prescribed sea surface only. Therefore, we focus here on 10m-wind speed only whereas the interested reader is referred to the RCA4-page
[http://www.smhi.se/en/Research/] for a detailed validation of RCA4.

Moreover, check section 5.4 to see how the 10m-wind speed is parametrized in RCA4. For a more detailed evaluation of the wind speed performance of RCA4 over the North Sea the reader is referred to *Kunne* [2012].

The direct comparison of wind speed measurements and simulated wind speed is difficult since observations are point measurements whereas the simulated wind speed reflects the average over an entire grid box. Moreover, no long-term observations exist over the open Baltic Sea so that coastal stations have to be used for a validation. However, wind speed gradients are especially strong along the coastline which makes it even more uncertain to directly compare measurements and simulations. For RCA3 a detailed validation was done by *Höglund et al.* [2009]. Here, this exercise is at least partly repeated for RCA4 data.

Fig. 24 shows the wind speed distribution of RCA4 and observations for Landsort (17.87°E, 58.74°N) and Lungo (18.09°E, 62.64°N) for a 10 year period. Generally speaking, the model and observations are in agreement. For Lungo high wind speeds are underestimated as in the former RCA3 version [*Höglund et al.*, 2009]. On the other hand, the wind speed distribution for Landsort is in better agreement with observations. Overall, a wind speed adjustment by the use of the gustiness seems not necessary anymore to drive an ocean model. This had to be done for the RCA3 wind speed [*Höglund et al.*, 2009].

Please note that a direct comparison of RCA3 and RCA4 data is not possible since the grid was shifted by half a grid box width. This has a strong impact on the points close to the coast which are validated here.

Finally, there are some differences in the distributions of the coupled and the uncoupled simulations. However, these differences are rather tiny.

The temporal evolution over a two months period of wind speed at Landsort is depicted in Fig. 25. It is obvious that both the coupled and uncoupled development of the wind speed is very similar. For this randomly chosen period

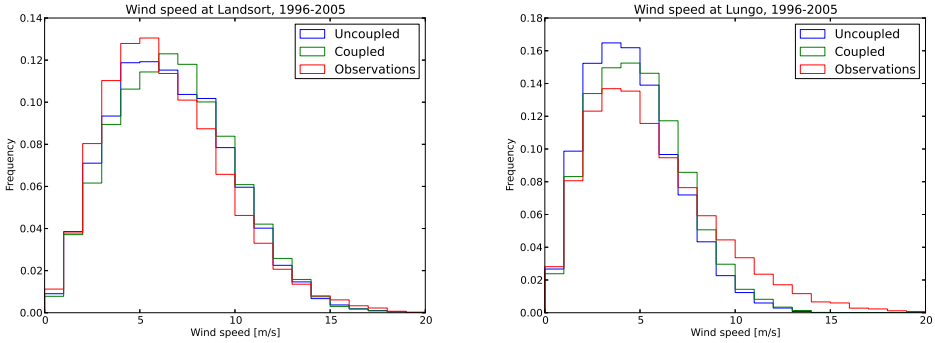

Figure 24: Wind speed histograms for Landsort and Lungo. The histograms include simulated wind speed from a coupled (green) and an uncoupled (blue) as well as observations (red). The distribution represents the period 1996–2005 which is common for all data sets.

the correlation exceeds 0.98. There is also general agreement with observations. However, the observations are characterized by stronger fluctuations.

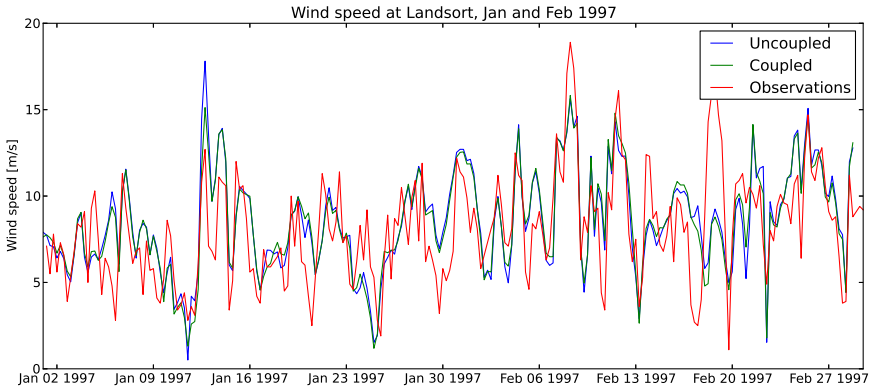

Figure 25: Wind speed evolution at Landsort for a two month period. The resolution is 3-hourly.

Finally, Fig. 26 is supposed to highlight the effect of the coupling. Namely, how the interactive feedback from the ocean effects the atmospheric wind field distribution. Therefore, the correlation coefficients between the uncoupled and coupled wind speed is computed for the entire model domain over a 10 year period. Since the same boundary data are used in both cases, the correlation is (almost) 1 in the relaxation zone of the model. Towards the inner part of the domain the correlation is decreasing but never falling below 0.8. Thereby,

lowest correlation occurs in the eastern part of the model. That is connected to the general westerly flow in the model domain. Tiny differences triggered over the coupled ocean areas can grow on its way downstream and peak close before leaving the model domain of the model. Moreover, a special effect can be seen over the Bothnian Bay and the Gulf of Finland. Here, the correlation is particular low which is in addition very restricted to the area over the sea. It is assumed that this is mainly connected to differences in modeled and prescribed ice cover which has a strong effect on the roughness length and heat fluxes.

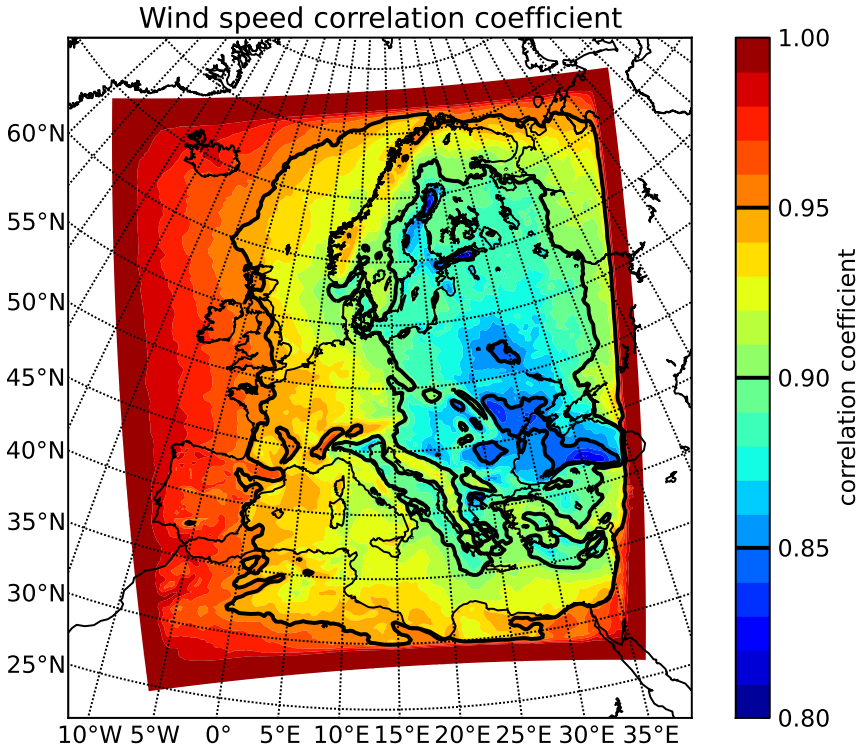

Figure 26: Correlation coefficients for the 10m-wind speed in the coupled and the uncoupled run. Correlations are computed using 3-hourly values for the period 1996–2005.

In summary, RCA4 coupled to NEMO seems to be very similar to RCA4 standalone at least for the 10m-wind speed. However, coupling effects might be larger for other parameters (e.g. precipitation) why a detailed analysis of ocean feedbacks onto the atmosphere will be presented in an additional paper.

5 Fluxes Coupling the Model Components

5.1 Shortwave Radiation

The modeled shortwave radiation is in general agreement with observations (Figs. 27+28). The seasonal cycle is well captured over the North and the Baltic Sea as shown as time series and monthly climatologies. One exception is the summer maximum which is underrepresented in the model. On the other side, the shortwave flux is somewhat overestimated during spring. The patterns for 1989 show that the absolute difference is typically below 10 W/m^2. Taking the mean shortwave radiation into account which is in the order of 100-125 W/m^2 the relative difference stays clearly under 10%.

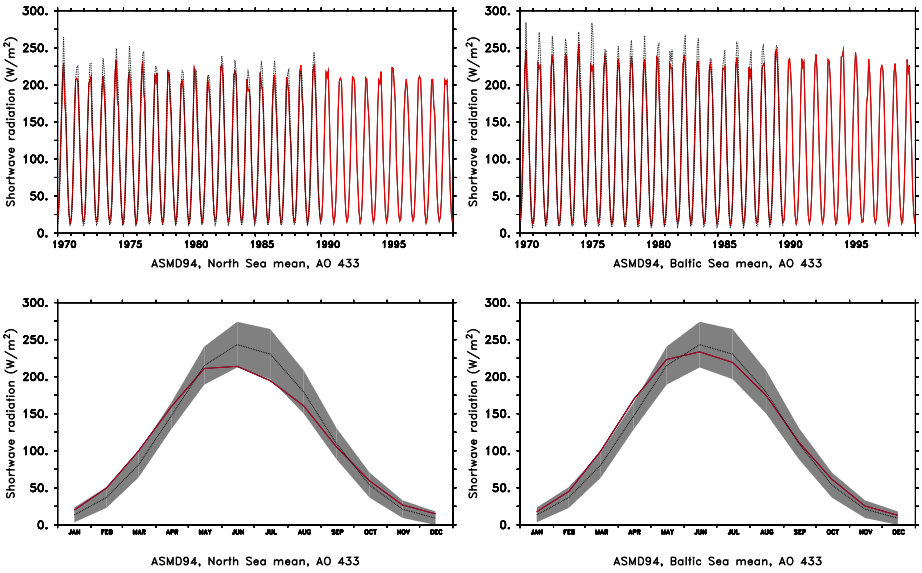

Figure 27: Shortwave radiation [W/m^2]: Top) Time series averaged over the North Sea (left) and the Baltic Sea (right). Observations (ASMD94) in black, model in red; Bottom) Mean seasonal cycle averaged over the North Sea (left) and the Baltic Sea (right), period 1970–1999.

However, even if the mean shortwave radiation is well simulated in RCA4 it remains to be validated that the radiation is handled in the right way in NEMO. Here, it seems clear already that some tuning needs to be done. So far many default settings are used for NEMO which are appropriate for global simulations. Consequently, there is the need to adapt this to match the characteristics of the North Sea and Baltic Sea.

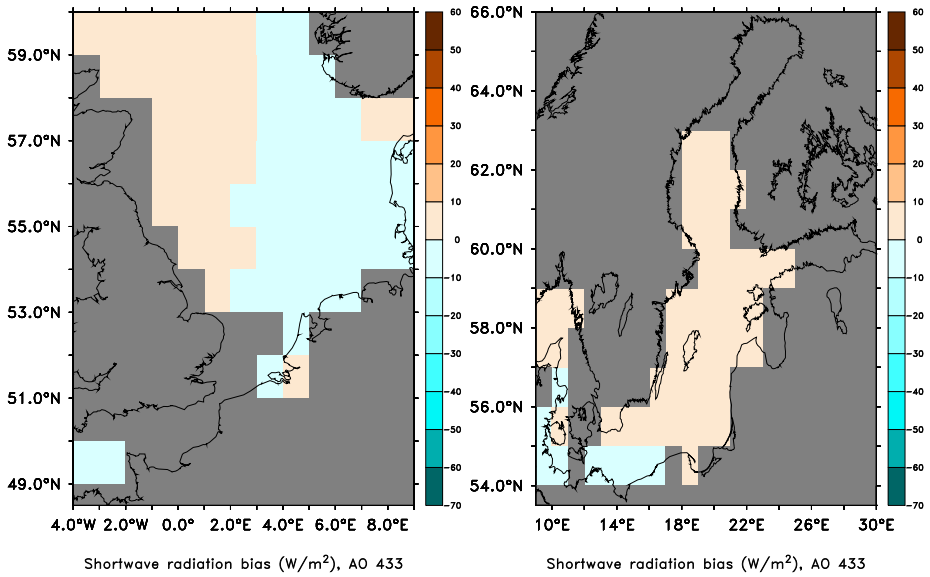

Figure 28: Shortwave radiation $[W/m^2]$ biases compared to ASMD94 observations for 1989 over the North Sea (left) and the Baltic Sea (right).

5.2 Non-solar Fluxes

The longwave radiation, sensible and latent heat fluxes are summarized as non-solar heat fluxes and compared to in-situ measurements (ASMD94, Fig. 29) and satellite derived estimates (HOAPS, Fig. 30). The inter-annual variability averaged over the North Sea and over the Baltic Sea are in reasonable agreement with the data. In a statistical sense the agreement is marginal. One estimate out of 20 estimates may lie outside the 95% confidence interval. For the Baltic Sea there are two out of twelve monthly means that are outside the confidence limits. Comparing model results with satellite derived estimates reveals that the ocean model transfers less heat to the atmosphere during the cold season.

5.3 Sea Surface Temperature

The sea surface temperatures in the ERA40 hindcast are in good agreement with the calibrated, satellite derived SST record by the BSH [*Loewe*, 1996; *Hoyer and She*, 2011]. Fig. 31 shows a comparison between modeled and observed SSTs for one specific year of a 16 year record of overlapping data (1990 - 2005). There is a tendency for the modeled SSTs to be too low, specially during summer. The 95% confidence interval supports the assumption that both realizations, the modeled as well as the observed are governed by the same process.

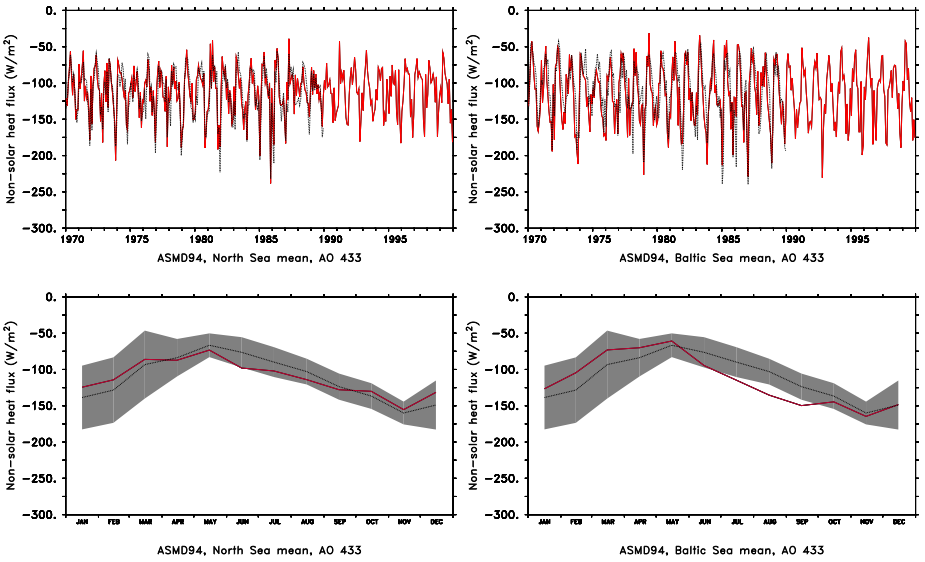

Figure 29: Non-solar flux $[W/m^2]$: Top) Time series averaged over the North Sea (left) and the Baltic Sea (right). Observations (ASMD94) in black, model in red; Bottom) Mean seasonal cycle averaged over the North Sea (left) and the Baltic Sea (right), period 1970–1999.

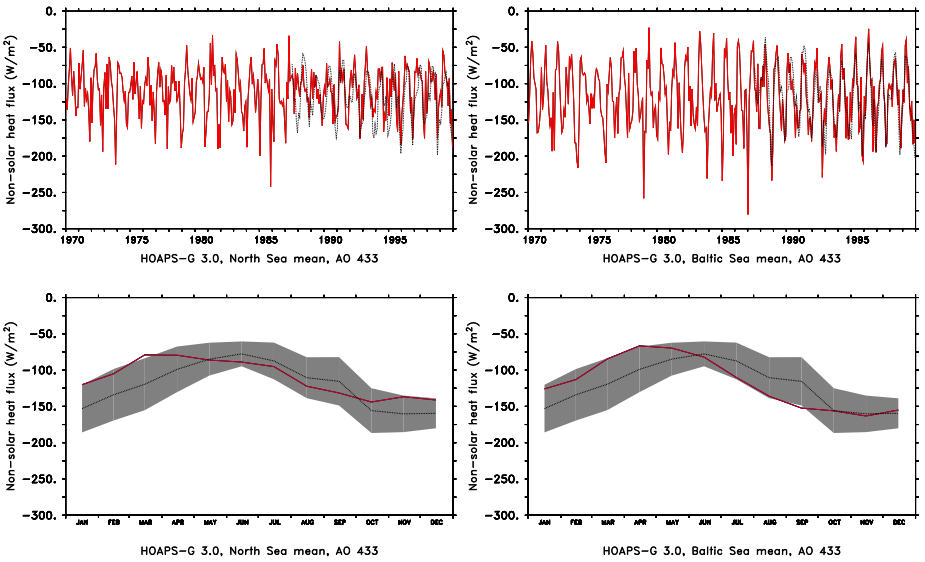

Figure 30: Same as Fig. 29 but with HOAPS data.

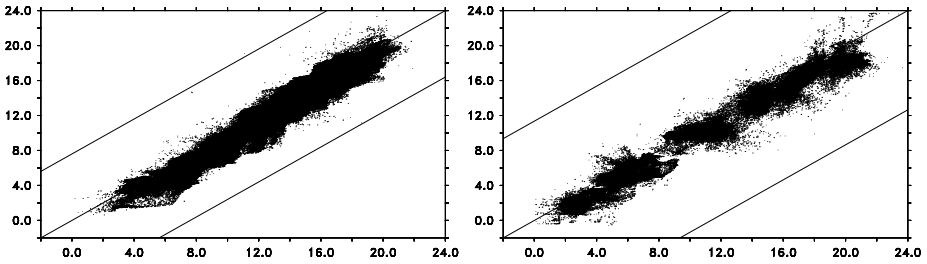

Figure 31: SST realizations for the year 1990 from the SST data-set of the BSH on the x-axis and from an ERA40 run with RCA4-NEMO on the y-axis. The two lines enclosing the data are the 95% confidence limits. North Sea (left) and Baltic Sea (right).

5.4 Wind Stress

Wind stress is the important forcing parameter for ocean currents in the North Sea and Baltic Sea (see section 4.1.1). In the coupled model the wind stress components are computed in RCA4, passed to NEMO and used directly. In contrast, 10m-wind speed is used as the forcing in the NEMO standalone version (BaltiX, *Hordoir et al.* [2013]) using bulk formulas to derive the wind stress. Since the atmospheric model has access to much more information, e.g. stability of the lower most atmosphere, one could assume that the wind stress computed by the atmospheric model should be more accurate than any wind stress based on the 10m-wind speed only. On the other hand, wind stress is not a well validated model parameter whereas atmospheric models are often tuned to reproduce the 10-wind speed fairly well. What is at the end the better parameter for the coupling is still under evaluation. However, it is clear that there are general differences between the methods. A short overview is given how the fluxes are computed in the next couple of lines.

The wind stress τ is defined as:

$$\tau = \rho u_*^2 f_m(Ri, z_a/z_0) = \rho C_D U_{z_a},$$

where u_* is the friction velocity, C_D is the neutral drag coefficient for momentum, U_{z_a} is the wind speed at lowest atmospheric model level z_a (at $\sim$30 m) and f_m is a correction factor for atmospheric stability, represented by the Richardson number Ri.

The neutral drag coefficient is defined as:

$$C_D = \frac{k^2}{\ln(z_a/z_0)},$$

where k is the von Karman's constant ($= 0.4$) and z_0 is the roughness length for momentum. The roughness length is defined as a function of wind speed interval:

$$z_0 = (1 - f_U)0.11\frac{\mu}{u_*} + f_U\alpha\frac{u_*^2}{g}.$$

Here $f_U = 0$ for $U_{z_a} < 3$ ms^{-1} and $f_U = 1$ for $U_{z_a} > 5$ ms^{-1} with a smooth transition in between. μ is the molecular kinematic viscosity of air ($= 1{\cdot}10^{-5}$), g is the acceleration of gravity and α is the Charnock constant. In coastal regions (where land is present in a grid box, at least 0.01%) we increase the roughness length of water by actually increasing the Charnock constant. Thus, over open sea $\alpha = 0.014$ while in coastal areas $\alpha = 0.032$.

Diagnostic variables of temperature and humidity at 2 m and wind at 10 m are calculated using Monin-Obukhov similarity theory [*Samuelsson et al.*, 2011].

Figure 32 depicts monthly means of easterly wind stress for two selected months. The top row shows the mean in January 1993 a month with particular strong westerly winds which caused also a major inflow event. The bottom row indicates the mean situation in January 1963 with general westerly wind stress in the southern Baltic and over the North Sea.

In general, the wind stress is substantially larger when computed directly with RCA4. That is true for the entire model domain but in particular for coastal regions (Fig. 32 top right).

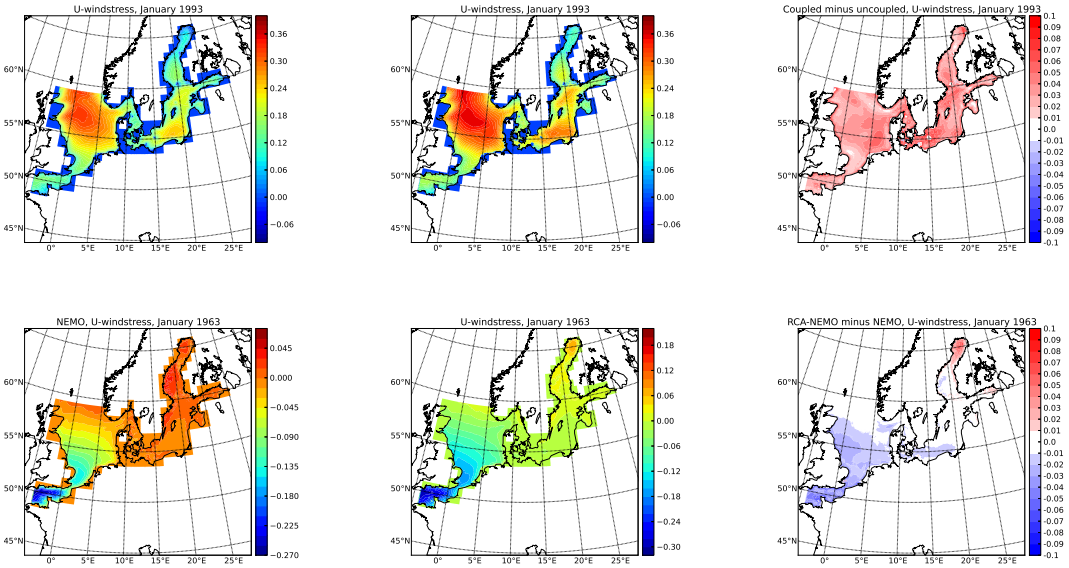

Figure 32: Easterly wind stress component for two selected events (January 1993 [top] and January 1963 [bottom]). Left) NEMO standalone; middle) NEMO coupled; right) difference between both.

A comparison to satellite based observations of wind stress in shown in

Fig. 33. For the most part colors are yellow to orange indicating a too strong wind stress in the coupled model. Consequently, wind stress based on the 10m-wind stress is closer to observations. However, as mentioned above it is still under investigations which parameter is most suitable for coupling the ocean model to the atmosphere model.

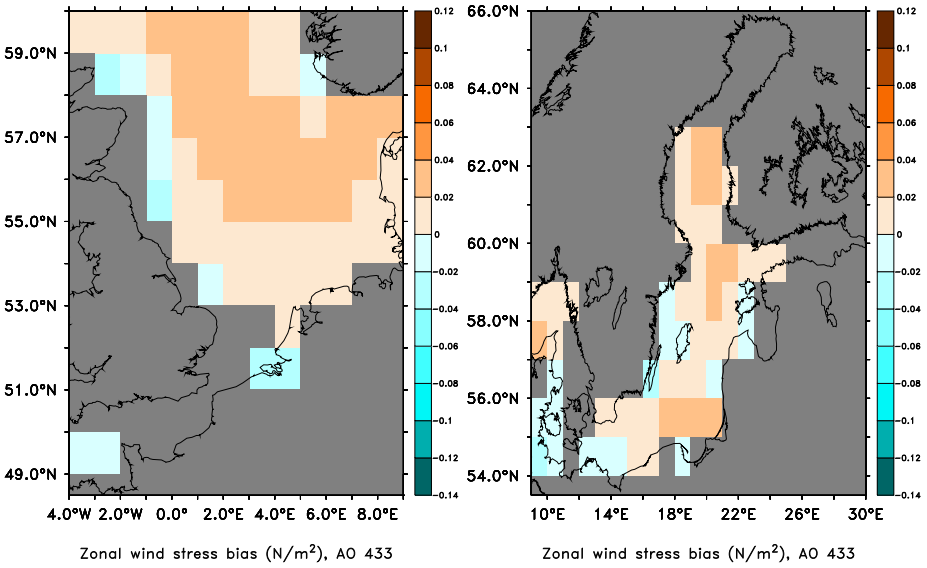

Figure 33: Difference between modeled and observed wind stress over the North Sea (left) and the Baltic Sea (right).

5.5 Freshwater Fluxes

The freshwater balance over open water is the difference between precipitation and evaporation. Since the North Sea and the Baltic Sea are located in the humid temperate climate zone the freshwater balance is generally positive. For the Baltic Sea, the mean net precipitation (evaporation minus precipitation, or short E-P) is estimated to roughly $-1.5 * 10^3 m^3/s$ based on observations [*Omstedt and Axell*, 2003]. Herewith, E-P add approximately 10% to the freshwater input into the Baltic Sea. RCA4-NEMO has $-1.1 * 10^3 m^3/s$ as a mean E-P value over the Baltic Sea what is in general agreement with observations.

Comparing model results with the Atlas of Surface Marine Data (ASMD94) [*Da Silva et al.*, 1996] it seems that E-P is especially underestimated during the cold season (Fig. 34 lower right). However, in comparison with HOAPS-G 3.0 data [*Andersson et al.*, 2007, 2010] model results appear much closer to observations.

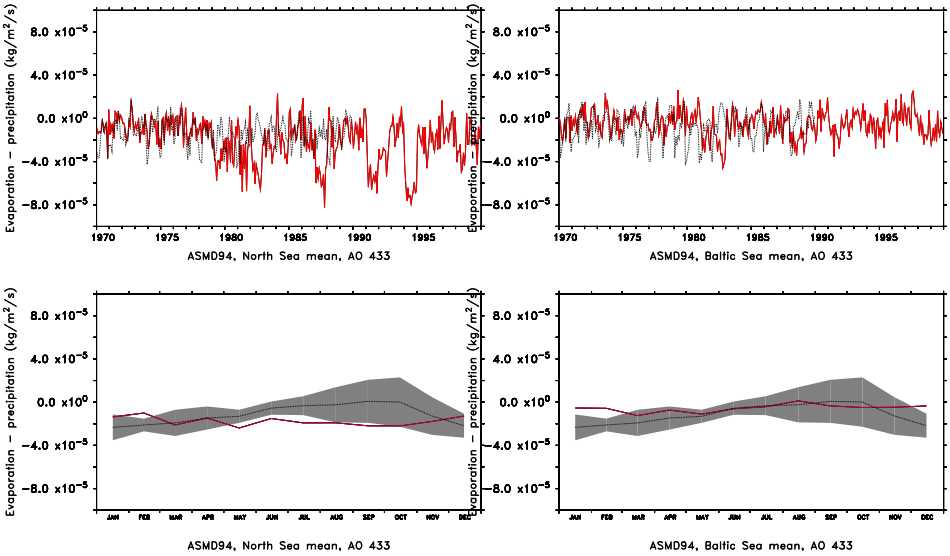

Figure 34: Evaporation minus precipitation $[kg/m^2/s]$: Top) Time series averaged over the North Sea (left) and the Baltic Sea (right). Observations (ASMD94) in black, model in red; Bottom) Mean seasonal cycle averaged over the North Sea (left) and the Baltic Sea (right), period 1970–1989.

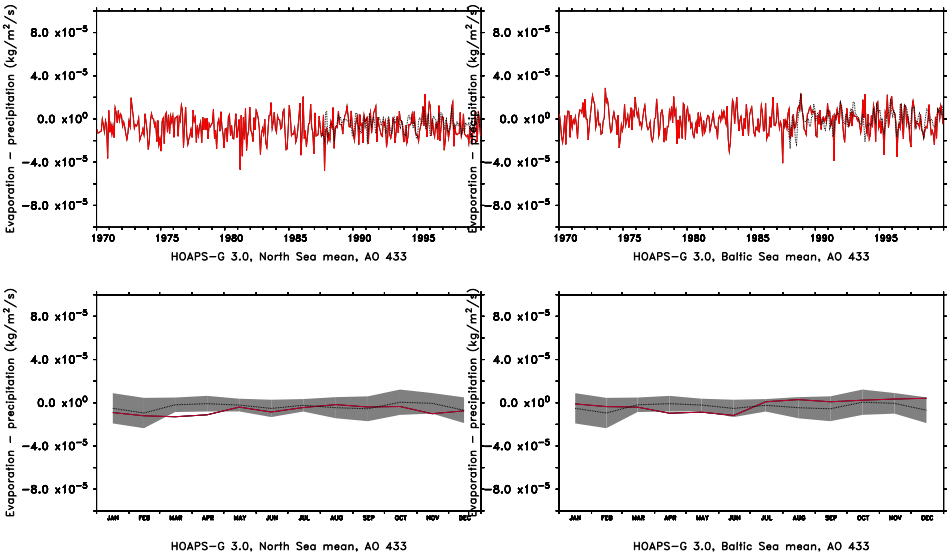

Figure 35: Same as Fig. 34 but with HOAPS data, period 1990–1999.

6 Summary

This report provides an evaluation of an ERA40 hindcast simulation carried out with the SMHI coupled atmosphere-ice-ocean model RCA4-NEMO. RCA4-NEMO is a regional climate model that is developed for process studies, hindcast simulations and for downscaling global climate change scenarios for the North Sea and Baltic Sea region.

International bodies like HELCOM [http://www.helcom.fi/] and OSPAR [http://www.ospar.org/] that aim to promote political decisions be made on the basis of scientific consensus will need estimates about the future development of the North Sea and Baltic Sea region. Regional earth system models like RCA4-NEMO do provide one possibility to extrapolate scientific knowledge about the climate system into the future.

To assess the validity of the present version of RCA4-NEMO we presented an analysis and discussion of an ERA40-driven downscaling experiment. This allows to compare model results directly with observations. Based on that comparison a number of shortcomings of the current model setup have been identified.

The comparison with climatologies yields satisfactory results, except for salinity in the ocean model component. This same comparison is carried out with the historical periods of scenario simulations that are used to downscale RCP [https://tntcat.iiasa.ac.at:8743/RcpDb/] scenarios from different GCMs.

The shortwave radiation was in general agreement with observations and the seasonal cycle well captured over the North Sea and the Baltic Sea. Non-solar heat fluxes agree both in statistical terms and in direct comparison with observations. The freshwater fluxes due to the net precipitation are somewhat underestimated during the cold season. The wind stress was substantially larger than in RCA4 standalone version, largest differences were found in coastal regions.

The hindcast results indicate that the physical properties of the North Sea and Baltic Sea are reasonably well simulated during the hindcast period, with the exception of salinity. The circulation patterns of the both regional seas are reproduced, but the circulation in the ocean model appears weaker than in other studies.

The inter-annual variability of the ice cover in the Baltic Sea is reproduced well compared to observations. The climatological ice cover during its maximum in February is underestimated in most parts of the Baltic Sea.

Outlook

RCA4-NEMO is actively being developed at the SMHI. The latest improvement was the implementation of a river routing scheme. To route the runoff from the atmosphere model back into the ocean model CaMa-Flood [*Yamazaki et al.*, 2011] has been coupled to the atmosphere-ice-ocean model using the OASIS3 coupler. This allows to run the RCM with a fully coupled water cycle. A first ERA40 simulation with CaMa-Flood looks very promising and validation

is under way.

The next steps in model development are aimed at eliminating the initial freshening of the North Sea in the ocean model component. Then a decision will be made about the question whether to pass wind stress or 10m wind from the atmosphere model to the ocean model. An open issue that needs to be addressed is the shallow and weak halocline in the Baltic Sea. The ice cover of the LIM3 model can be made to match the climatological maps compiled from observations by reducing the diffusivity of the ice. This will be tested in future model runs. On the technical side there is some potential to improve the performance of RCA4-NEMO to save computational resources.

The next short-term goal is to include an adapted version of the Swedish Coastal and Ocean BIogeochemical model (SCOBI) into the NEMO code and add the next component on the way to a regional earth system model for the North Sea and Baltic Sea region.

Acknowledgments

We would like to thank Patrick Samuelsson for contributing the details about the implementation of wind stress calculations in RCA4.

Katharina Bülow and Birgit Klein made available the MARNET data in electronic form.

The modeling effort presented in this report has been funded by the KLIWAS [http://kliwas.de/] program. KLIWAS - Impacts of Climate Change on Waterways and Navigation is a joint research program of the German Federal Institute of Hydrology (BfG), the German Federal Waterways and Engineering and Research Institute (BAW), the National Weather Service of Germany (DWD) and the Federal Maritime and Hydrographic Agency (BSH) in co-operation with universities and other research institutions. KLIWAS is funded by the Federal Ministry of Transport, Building and Urban Development (BMVBS).

The coupled model runs with RCA4-NEMO have been conducted on the Linux clusters Krypton and Triolith, both operated by the NSC [http://www.nsc.liu.se/]. Resources on the Linux cluster Triolith have been made available by the grant SNIC 002/12-25 "Regional climate modeling for the North Sea and Baltic Sea regions". This part of the simulations were performed on resources provided by the Swedish National Infrastructure for Computing (SNIC) at the National Supercomputer Centre in Sweden (NSC).

7 Bibliography

Alenius, P., K. Myrberg, and A. Nekrasov, The physical oceanography of the Gulf of Finland: a review, *Boreal Environment Research*, *3*, 97–125, 1998.

Andersson, A., S. Bakan, K. Fennig, H. Grassl, C. Klepp, , and J. Schulz, Hamburg Ocean Atmosphere Parameters and Fluxes from Satellite Data - HOAPS-3 - monthly mean, in *electronic publication*, World Data Center for Climate, 2007.

Andersson, A., K. Fennig, C. Klepp, S. Bakan, H. Grassl, and J. Schulz, The Hamburg Ocean Atmosphere Parameters and Fluxes from Satellite Data - HOAPS-3, *Earth Syst. Sci. Data*, *2*, 215–234, 2010.

Andrejev, O., K. Myrberg, P. Alenius, and P. A. Lundberg, Mean circulation and water exchange in the Gulf of Finland – a study based on three-dimensional modelling, *Boreal Environment Research*, *9*, 1–16, 2004.

BACC, *Assessment of Climate Change for the Baltic Sea Basin*, Springer, 2008.

Bechtold, P., E. Bazile, F. Guichard, P. Mascart, and E. Richard, A mass convection scheme for regional and global models, *Q. R. J. Meteorol. Soc.*, *127*, 869–886, 2001.

Becker, G. A., and M. Pauly, Sea surface temperature changes in the North Sea and their causes, *ICES Journal of Marine Science*, *53*, 887–898, 1996.

Berx, B., and S. Hughes, Climatology of Surface and Near-bed Temperature and Salinity on the North-West European Continental Shelf for 1971-2000, *Continental Shelf Research*, *29*, 2286–2292, 2009.

Bouillon, S., M. A. M. Maqueda, V. Legat, and T. Fichefet, An elastic-viscous-plastic sea ice model formulated on Arakawa B and C grids, *Ocean Modelling*, *27*, 174–184, 2009.

Curry, J. A., J. L. Schramm, and E. E. Ebert, Sea Ice-Albedo Climate Feedback Mechanism, *J. Climate*, *8*, 240–247, 1995.

Da Silva, A., C. Young-Molling, and S. Levitus, Revised surface marine fluxes over the global oceans: the UWM/COADS data set, in *WCRP Workshop on Air–Sea Flux Fields for Forcing Ocean Models and Validating GCMS*, edited by G. White, 762, pp. 13–18, WMO, 1996.

Döscher, R., and A. Beckmann, Effects of a bottom boundary layer parameterization in a coarse-resolution model of the North Atlantic ocean, *J. Atmos. Ocean. Technol.*, *17*, 698–707, 2000.

Döscher, R., U. Willén, C. Jones, A. Rutgersson, H. Meier, U. Hansson, and L. Graham, The development of regional coupled ocean-atmosphere model RCAO, *Boreal Env. Res.*, *7*, 183–192, 2002.

Egbert, G. D., and S. Y. Erofeeva, Efficient inverse modeling of barotropic ocean tides, *J. Atmos. Ocean. Technol.*, *19*, 183–204, 2002.

Goedecke, E., J. Smed, and G. Tomczak, Monatskarten des Salzgehaltes der Nordsee dargestellt fuer verschiedene Tiefenhorizonte, *Ergänzungsheft zur Deutschen Hydrographischen Zeitschrift 9*, Deutsches Hydrographisches Institut, Hamburg, 1967.

Gustafsson, N., L. Nyberg, and A. Omstedt, Coupling of a High-Resolution Atmospheric Model and an Ocean Model for the Baltic Sea, *Mon. Wea. Rev.*, *126*, 2822–2846, 1998.

Hagedorn, R., A. Lehmann, and D. Jacob, A coupled high resolution atmosphere-ocean model for the BALTEX region, *Meteorologische Zeitschrift*, *9*, 7–20, 2000.

Ho, H. T. M., B. Rockel, H. Kapitza, B. Geyer, and E. Meyer, COSTRICE – three model online coupling using OASIS: problems and solutions, *Geoscientific Model Development Discussions*, *5*, 3261–3310, 2012.

Höglund, A., H. M. Meier, B. Broman, and E. Kriezi, Validation and correction of regionalised ERA-40 wind fields over the Baltic Sea using the Rossby Centre Atmosphere model RCA3.0, *Report Oceanografi 97*, SMHI, 2009.

Hordoir, R., B. W. An, J. Haapala, C. Dieterich, S. Schimanke, A. Höglund, and H. M. Meier, BaltiX: A 3D Ocean Modelling Configuration for Baltic & North Sea Exchange Analysis, *Report Oceanography 48*, SMHI, 2013.

Hoyer, J. L., and J. She, Validation of satellite SST products for the North Sea-Baltic Sea region, *Technical Report 04-11*, DMI, Copenhagen, Denmark, 2011.

Hunke, E., and J. Dukowicz, An elastic-viscous-plastic model for sea ice dynamics, *Journal of Physical Oceanography*, *27*, 1849–1867, 1997.

Janssen, F., C. Schrum, and J. O. Backhaus, A Climatological Data Set of Temperature and Salinity for the Baltic Sea and the North Sea, *Hydrographische Zeitschrift German Journal of Hydrography*, *Supplement*, 245 pp, 1999.

Jones, C., U. Willen, A. Ullerstig, and U. Hansson, The Rossby Centre regional atmospheric climate model part I: model climatology and performance for the present climate over Europe, *Ambio*, *33*, 199–210, 2004.

Jones, P. W., First- and second-order conservative remapping schemes for grids in spherical coordinates, *Mon. Wea. Rev.*, *127*, 2204–2210, 1999.

Kain, J., and J. Fritsch, *Convective parameterisations for mesocale models: The Kain-Fritsch scheme. In: The Representation of Cumulus Convection in Numerical Models*, American Meteorological Society Monograph, Boston, USA, 1993.

Käse, R. H., J. B. Girton, and T. B. Sanford, Structure and variability of the Denmark Strait Overflow: Model and observations, *J. Geophys. Res.*, *108*, 15 p, 2003.

Krauss, W., and B. Brügge, Wind-produced water exchange between the deep basins of the Baltic Sea, *Journal of Physical Oceanography*, *21*, 373–384, 1991.

Kunne, B., Eavaluation of the Wind Field Distribution in the Rossby Centre Regional Climate Model RCA4 over the North Sea for 1979-2010, *Tech. rep.*, SMHI, Rossby Centre, 2012.

Lehmann, A., and H.-H. Hinrichsen, Water, heat and salt exchange between the deep basins of the Baltic Sea, *Boreal Environment Research*, *7*, 405–415, 2002.

Lehmann, A., W. Krauss, and H. H. Hinrichsen, Effects of remote and local atmospheric forcing on circulation and upwelling in the Baltic Sea, *Tellus A*, *54*, 299–316, 2002.

Levier, B., A.-M. Tréguier, G. Madec, and V. Garnier, Free surface and variable volume in the nemo code, *Tech. rep. MERSEA IP report WP09-CNRSSTR-03-1A,*, MERSEA, available on the NEMO web site, 2007.

Levitus, S., and T. P. Boyer, World Ocean Atlas 1994. Volume 4: Temperature, *NOAA Atlas NESDIS 4*, NOAA, Washington D.C., 1994.

Levitus, S., R. Burgett, and T. P. Boyer, World Ocean Atlas 1994. Volume 3: Salinity, *NOAA Atlas NESDIS 3*, NOAA, Washington D.C., 1994.

Lindström, G., C. Pers, J. Rosberg, J. Strömqvist, and B. Arheimer, Development and testing of the HYPE (Hydrological Predictions for the Environment) water quality model for different spatial scales, *HYDROLOGY RESEARCH*, *41*, 295–319, 2010.

Liu, Y., H. M. Meier, and L. Axell, Reanalyzing temperature and salinity on decadal time scales using a 3d ocean circulation model of the Baltic Sea, *JGR*, *submitted*, 2013.

Loewe, P., Surface temperatures of the North Sea in 1996, *Ocean Dynamics*, *48*, 175–184, 1996.

Madec, G., NEMO ocean engine, *User Manual 3.3*, IPSL, Paris, France, 2011.

Martynov, A., L. Sushama, and R. Laprise, Simulation of temperate freezing lakes by one-dimensional lake models: performance assessment for interactive coupling with regional climate models, *Boreal Env. Res.*, *15*, 143–164, 2010.

Matthäus, W., and H. Franck, Characteristics of major Baltic inflows - a statistical analysis, *Continental Shelf Research*, *12*, 1375 – 1400, 1992.

Matthäus, W., and H. Schinke, Mean atmospheric circulation patterns associated with major Baltic inflows, *Deutsche Hydrografische Zeitschrift*, *46*, 321–339, 1994.

Meier, H. E. M., Modeling the pathways and ages of inflowing salt- and freshwater in the Baltic Sea, *Estuarine Coastal Shelf Sci.*, *74*, 717–734, 2007.

Meier, H. E. M., R. Döscher, and T. Faxén, A multiprocessor coupled ice-ocean model for the Baltic Sea: Application to salt inflow, *J. Geophys. Res.*, *108*, 29 p, 2003.

Mironov, D., E. Heise, E. Kourzeneva, B. Ritter, N. Schneider, and A. Terzhevik, Implementation of the lake parameterisation scheme FLake into the numerical weather prediction model COSMO, *Boreal Env. Res.*, *15*, 218–230, 2010.

Mironov, D. V., Parameterization of lakes in numerical weather prediction. description of a lake model, *COSMO Technical Report 11*, Deutscher Wetterdienst, Offenbach am Main, 2008.

Myrberg, K., and O. Andrejev, Modelling of the circulation, water exchange and water age properties of the Gulf of Bothnia, *Oceanologia*, *48(S)*, 55–74, 2006.

Omstedt, A., and L. Axell, Modeling the variations of salinity and temperature in the large Gulfs of the Baltic Sea, *Continental Shelf Research*, *23*, 265–294, 2003.

Orlanski, I., A simple boundary condition for unbounded hyperbolic flows, *J. Comp. Phys*, *21*, 251 – 269, 1976.

Pirazzini, R., Challenges in snow and ice albedo parameterizations, *Geophysica,*, *45*, 41–62, 2009.

Robock, A., The seasonal cycle of snow cover, sea ice and surface albedo, *Mon. Wea. Rev.*, *108*, 267–285, 1980.

Rummukainen, M., J. Risnen, B. Bringfelt, A. Ullerstig, and co authors, A regional climate model for northern Europe: model description and results from the downscaling of two GCM control simulations, *Climate Dynamics*, *17*, 339–359, 2001.

Samuelsson, P., et al., The Rossby Centre Regional Climate model RCA3: model description and performance, *Tellus*, *63A*, 4–23, 2011.

Schrum, C., U. Hübner, D. Jacob, and R. Podzun, A coupled atmosphere/ice/ocean model for the North Sea and Baltic Sea, *Climate Dynamics*, *21*, 131–151, 2003.

Smagorinsky, J., General Circulation Experiments with the Primitve Equations: 1 the Basic Experiment, *Mon. Wea. Rev.*, *91*, 99–164, 1963.

Sündermann, J., and T. Pohlmann, A brief analysis of North Sea physics, *Oceanologia*, *53(3)*, 663–689, 2011.

Tian, T., F. Boberg, O. Christensen, J. Christensen, J. She, and T. Vihma, Simulations of the last two decades Baltic Sea climate using a high-resolution regional climate model: a comparison using prescribed and modelled SSTs, *Tellus*, *submitted*, 2013.

Tomczak, G., and E. Goedecke, Die thermische Schichtung der Nordsee auf Grund des mittleren Jahresganges der Temperatur in 1/2 °- und 1 °- Feldern, *Ergänzungsheft zur Deutschen Hydrographischen Zeitschrift 8*, Deutsches Hydrographisches Institut, Hamburg, 1964.

Udin, I., J. Sahlberg, and M. Leppäranta, Climatological ice atlas for the Baltic Sea, Kattegat, Skagerrak and Lake Vänern (1963-1979), *Technical Report 04-11*, SMHI, Norrköping, Sweden, 1982.

Unden, P., et al., Hirlam-5 scientific documentation, *Tech. rep.*, Swedish Meteorological and Hydrological Institute (SMHI), Sweden, Norrkping, 2002.

Uppala, S. M., et al., The ERA-40 re-analysis, *Quaterly Journal of the Royal Meteorological Society*, *131*, 2961–3012, 2005.

Valcke, S., OASIS3 User Guide, *Technical Report TR/CMGC/06/73, PRISM Report No 3*, CERFACS, Toulouse, France, 2006.

Valcke, S., The OASIS3 coupler: a European climate modelling community software, *Geoscientific Model Development Discussions*, *5*, 2139–2178, 2012.

Vancoppenolle, M., T. Fichefet, H. Goosse, S. Bouillon, G. Madec, and M. A. M. Maqueda, Simulating the mass balance and salinity of arctic and antarctic sea ice, *Ocean Modelling*, *27*, 33–53, 2009.

Vranes, K., A. L. Gordon, and A. Ffield, The heat transport of the Indonesian Throughflow and implications for the Indian Ocean heat budget, *Deep–Sea Res. II*, *49*, 1391–1410, 2002.

Winther, N., and J. Johannessen, North Sea circulation: Atlantic inflow and its destination, *Journal of Geophysical Research*, *111*, 1–12, 2006.

Yamazaki, D., S. Kanae, H. Kim, and T. Oki, A physically based description of floodplain inundation dynamics in a global river routing model, *Water Resource Research*, *47*, 21 pp, 2011.

A Additional Figures

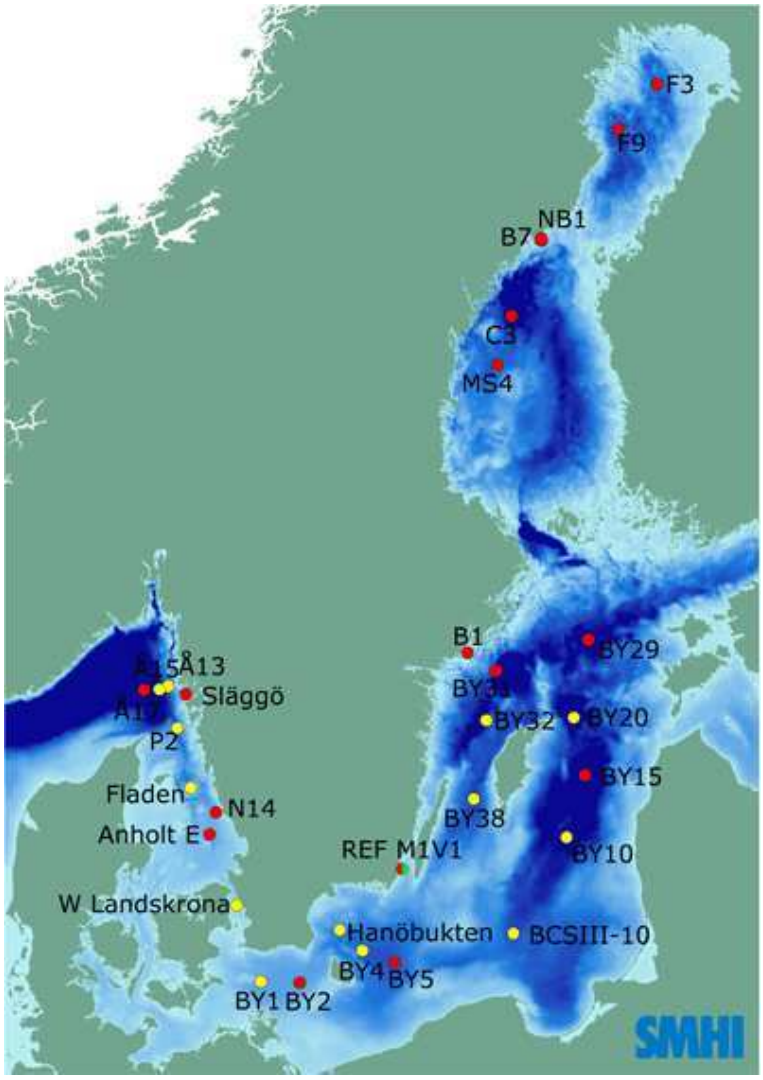

Figure 36: Locations of observational stations used in the following figures.

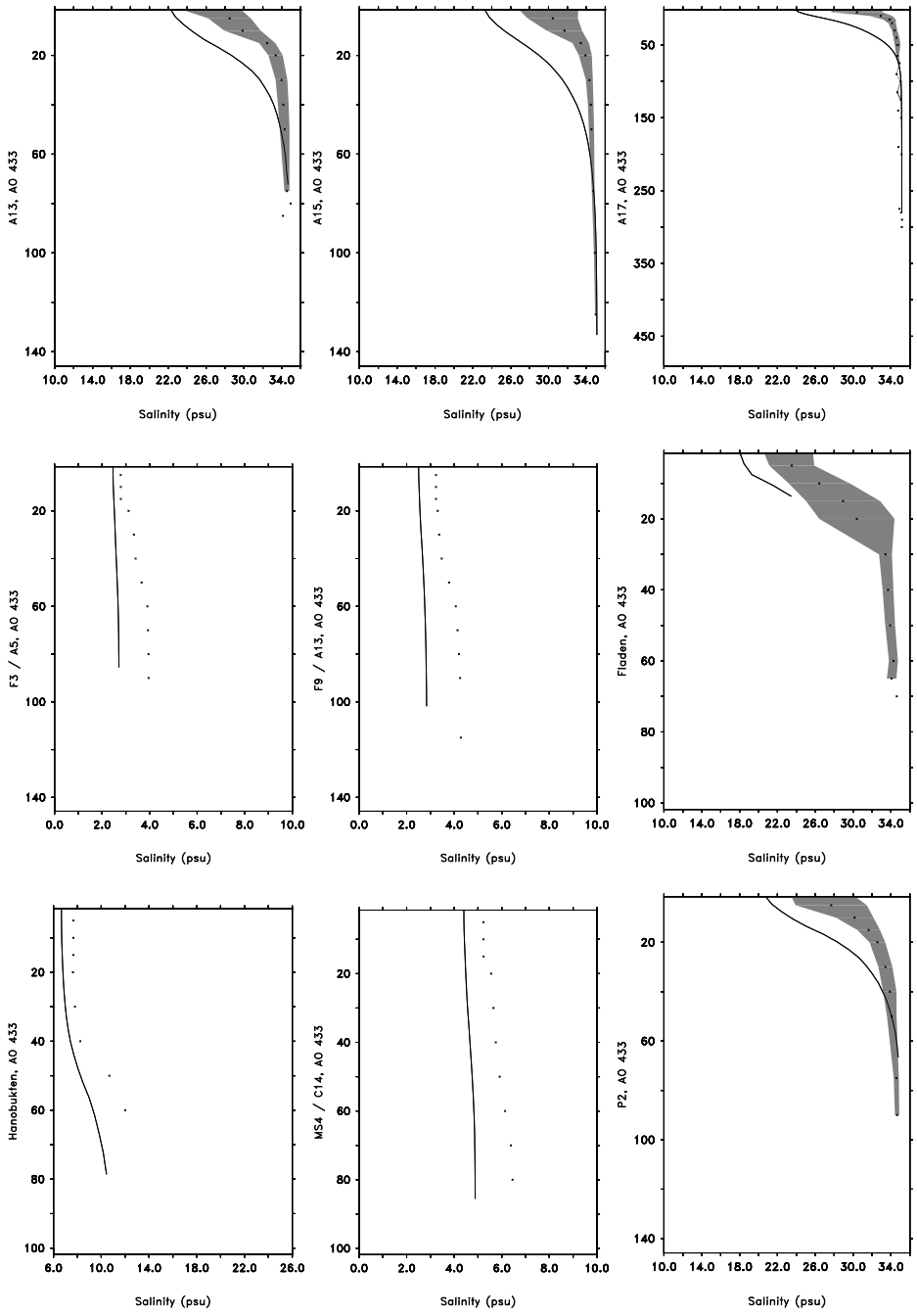

Figure 37: Salinity profiles at stations throughout the model domain. Dots indicate measurements and the solid line model results.

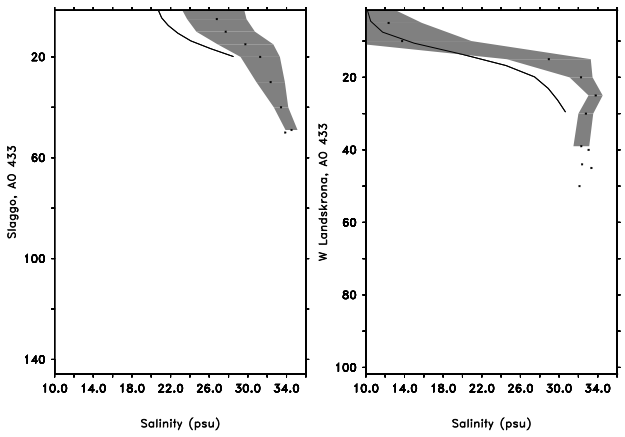

Figure 38: Salinity profiles at stations throughout the model domain. Dots indicate measurements and the solid line model results.

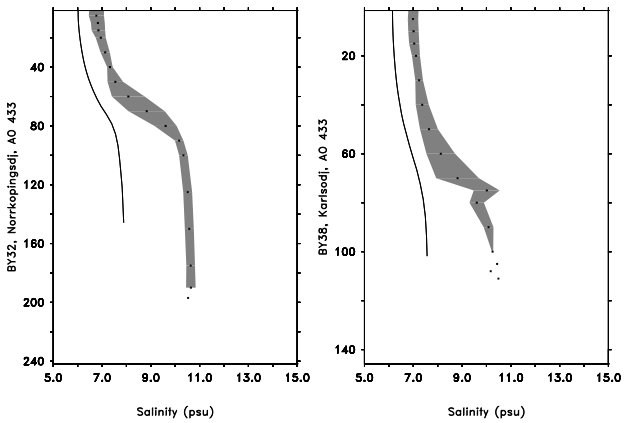

Figure 39: Salinity profiles at stations throughout the model domain. Dots indicate measurements and the solid line model results.

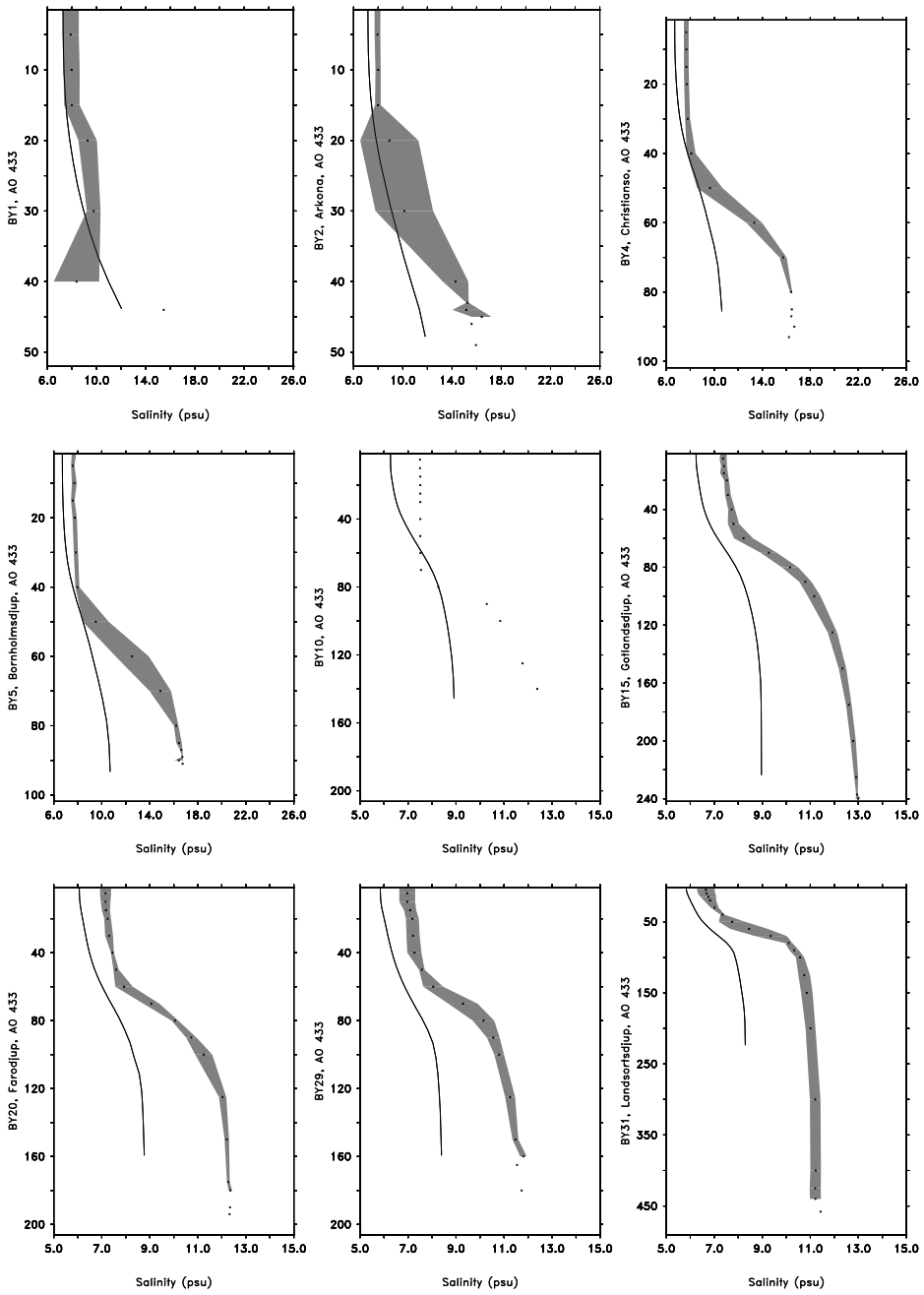

Figure 40: Salinity profiles at stations throughout the model domain. Dots indicate measurements and the solid line model results.

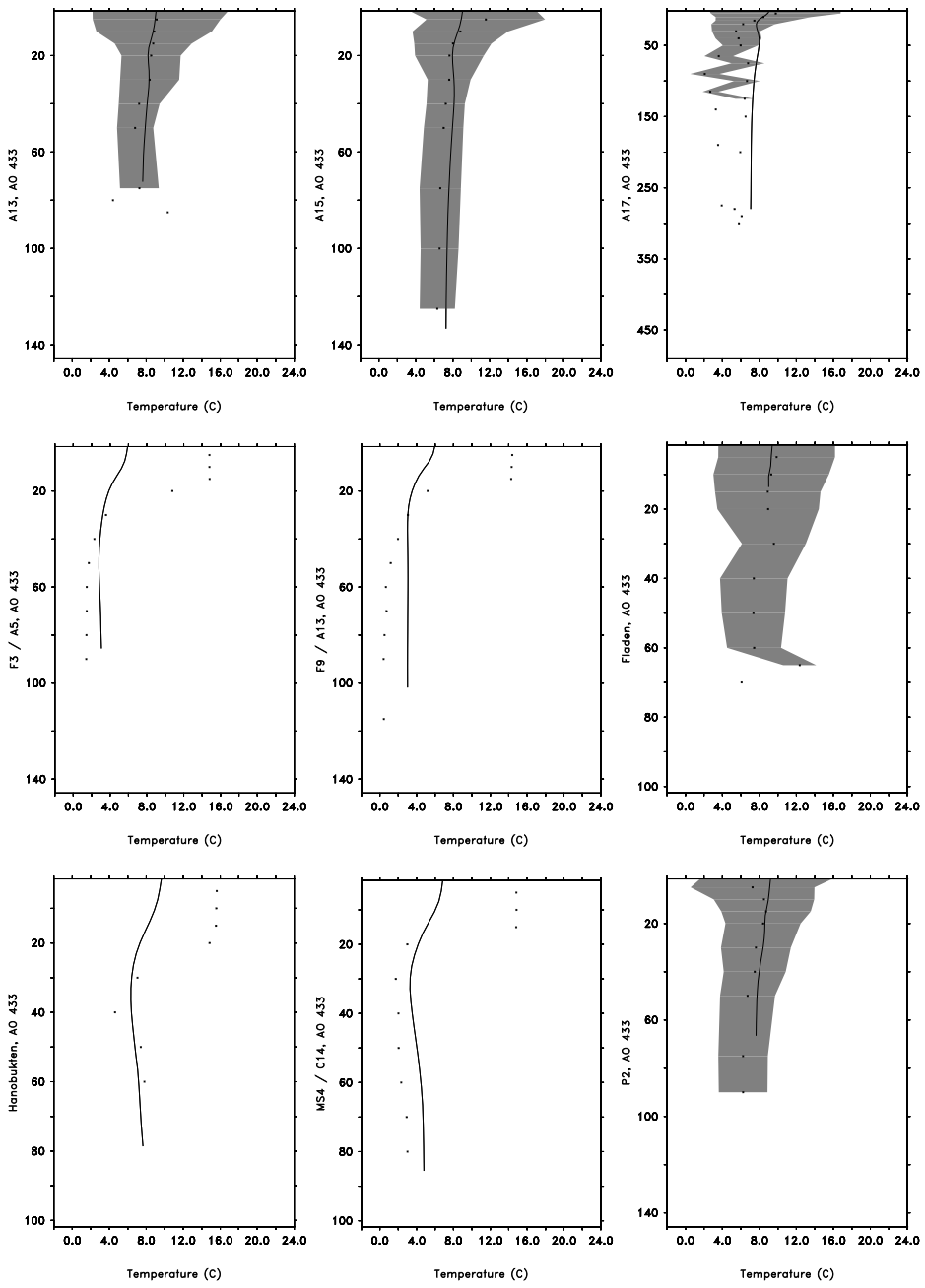

Figure 41: Temperature profiles at stations throughout the model domain. Dots indicate measurements and the solid line model results.

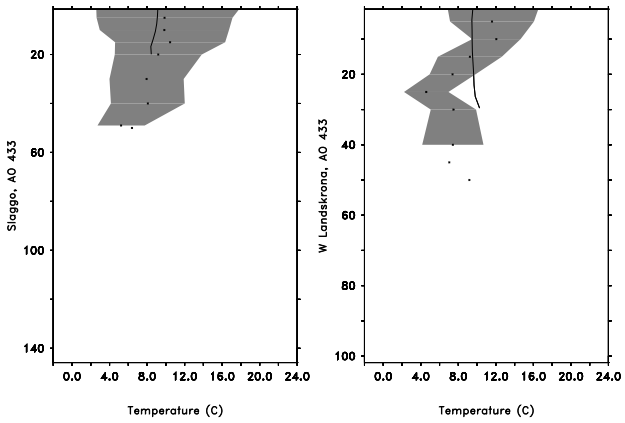

Figure 42: Temperature profiles at stations throughout the model domain. Dots indicate measurements and the solid line model results.

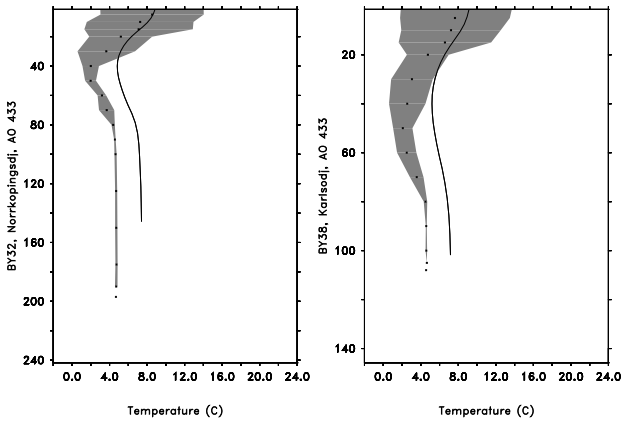

Figure 43: Temperature profiles at stations throughout the model domain. Dots indicate measurements and the solid line model results.

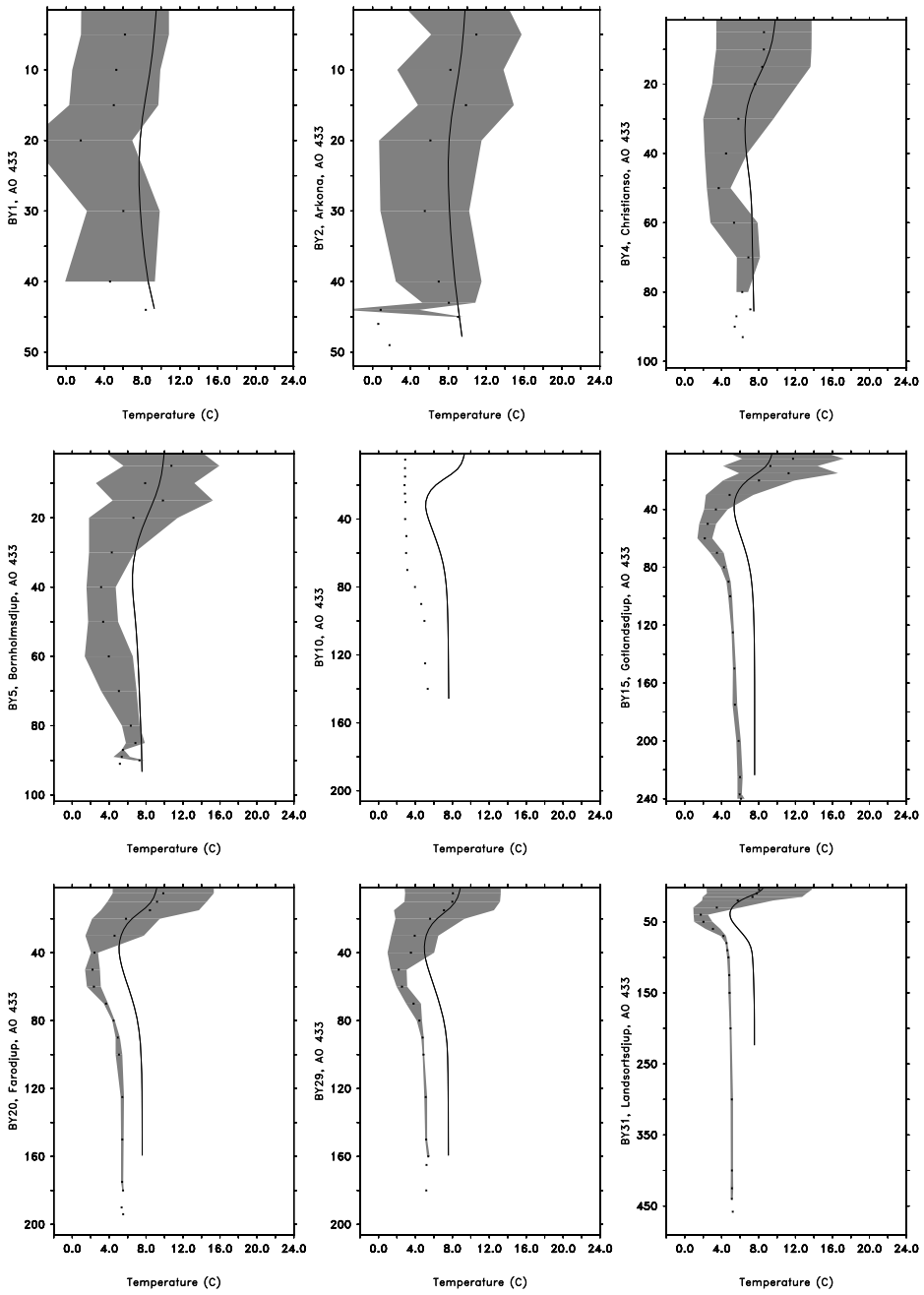

Figure 44: Temperature profiles at stations throughout the model domain. Dots indicate measurements and the solid line model results.

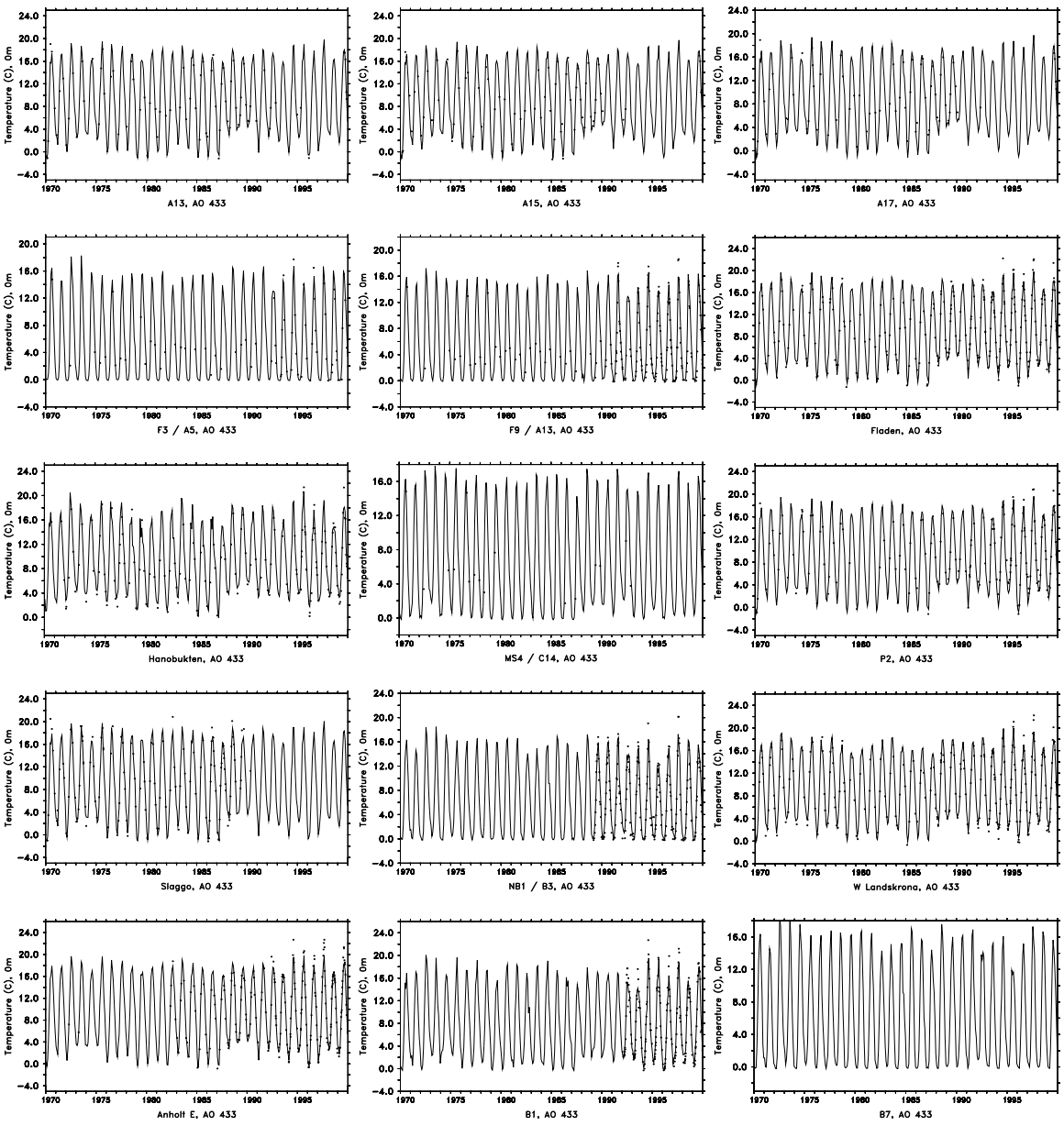

Figure 45: SST series at stations throughout the model domain. Dots indicate measurements and the solid line model results.

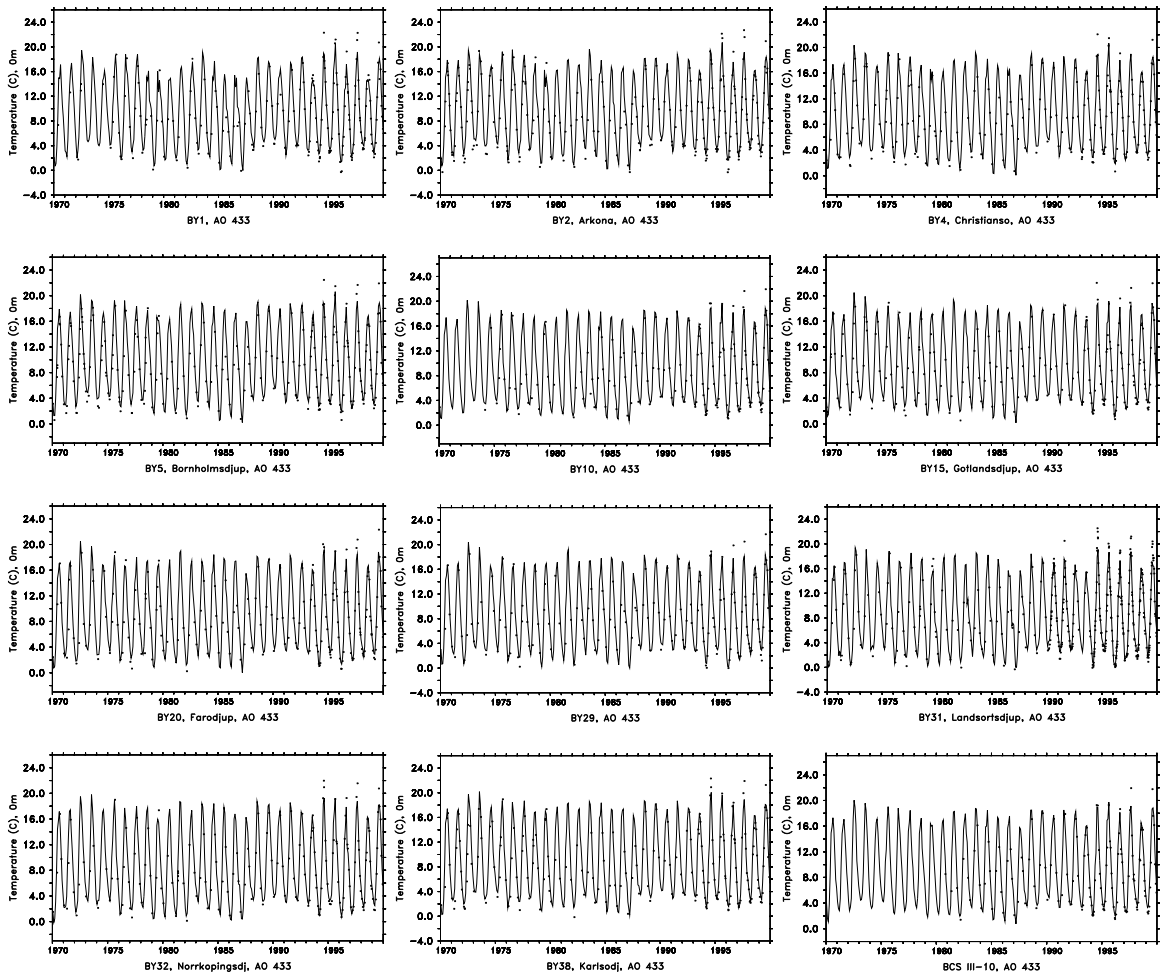

Figure 46: SST series at stations throughout the model domain. Dots indicate measurements and the solid line model results.

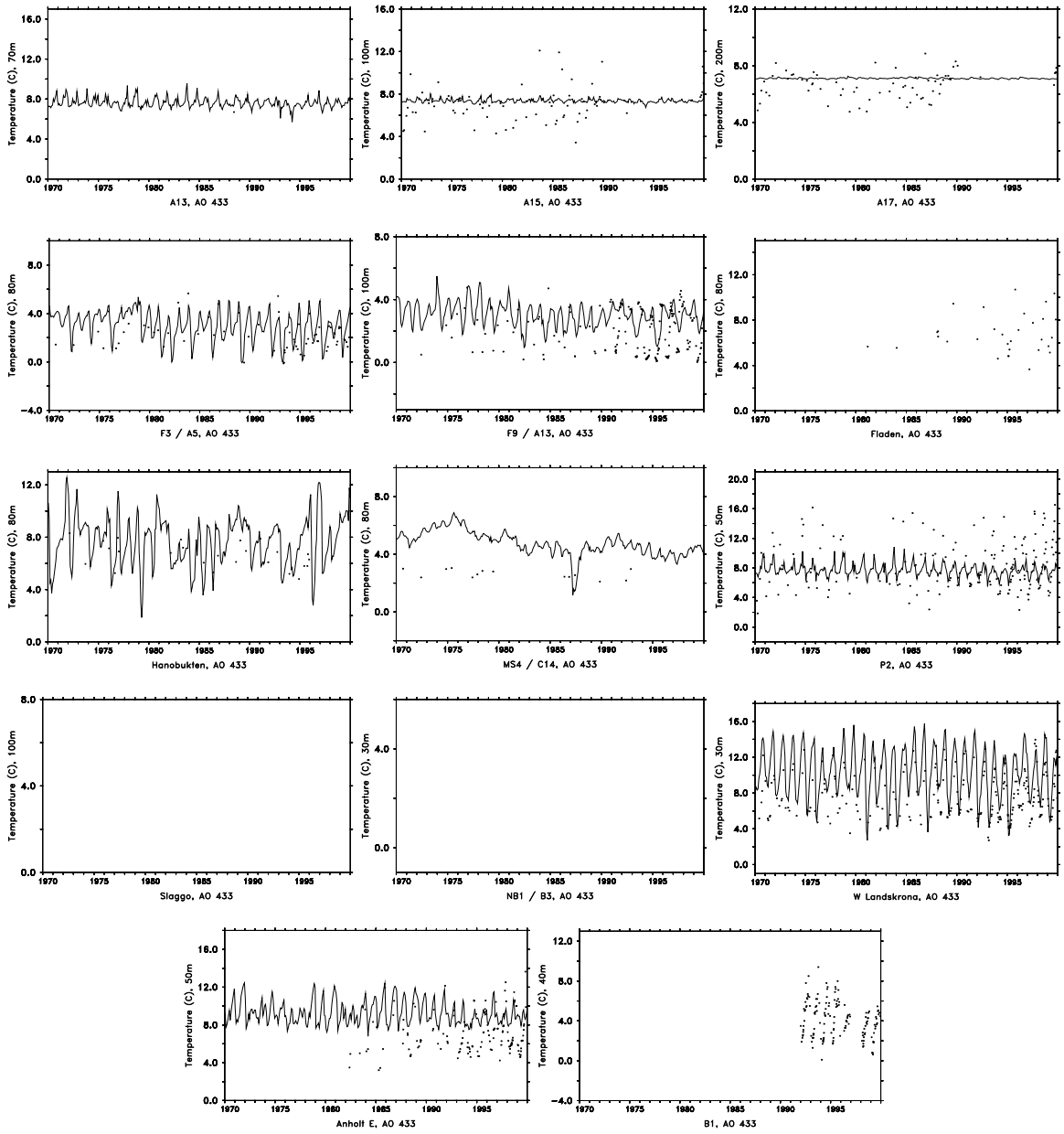

Figure 47: Temperature series at near bottom model levels for locations with observations. Dots indicate measurements and the solid line model results.

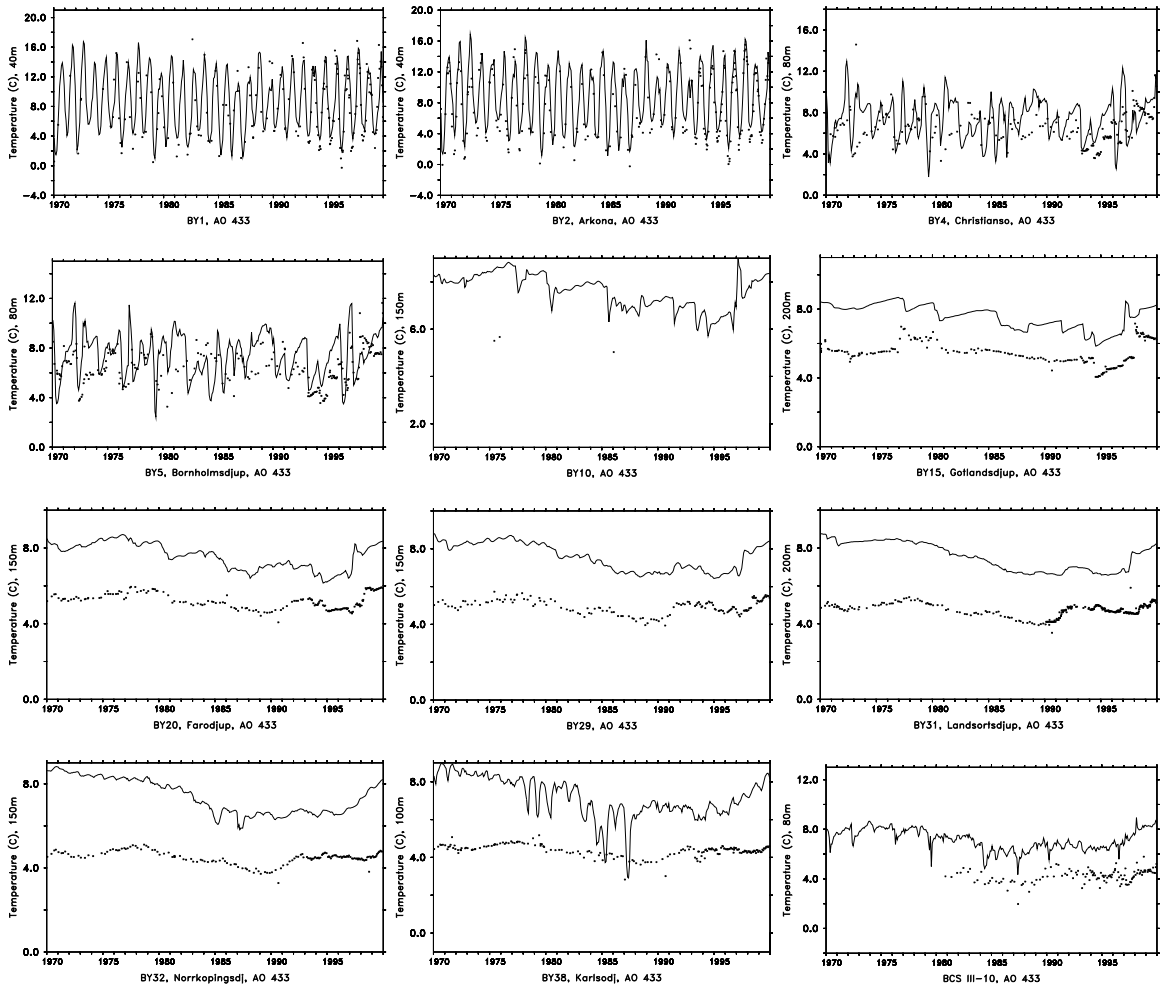

Figure 48: Temperature series at near bottom model levels for locations with observations. Dots indicate measurements and the solid line model results.

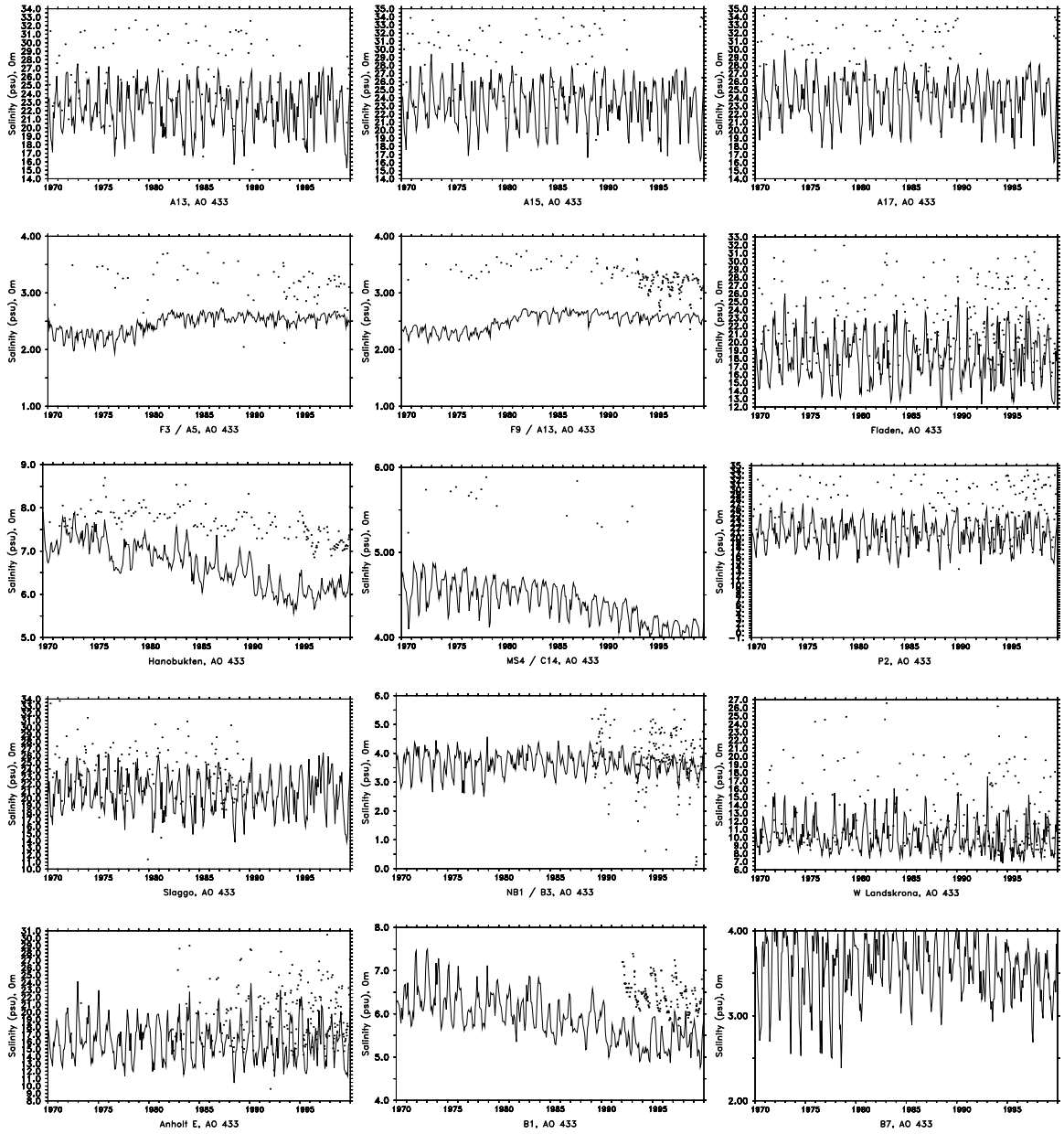

Figure 49: SSS series at stations throughout the model domain. Dots indicate measurements and the solid line model results.

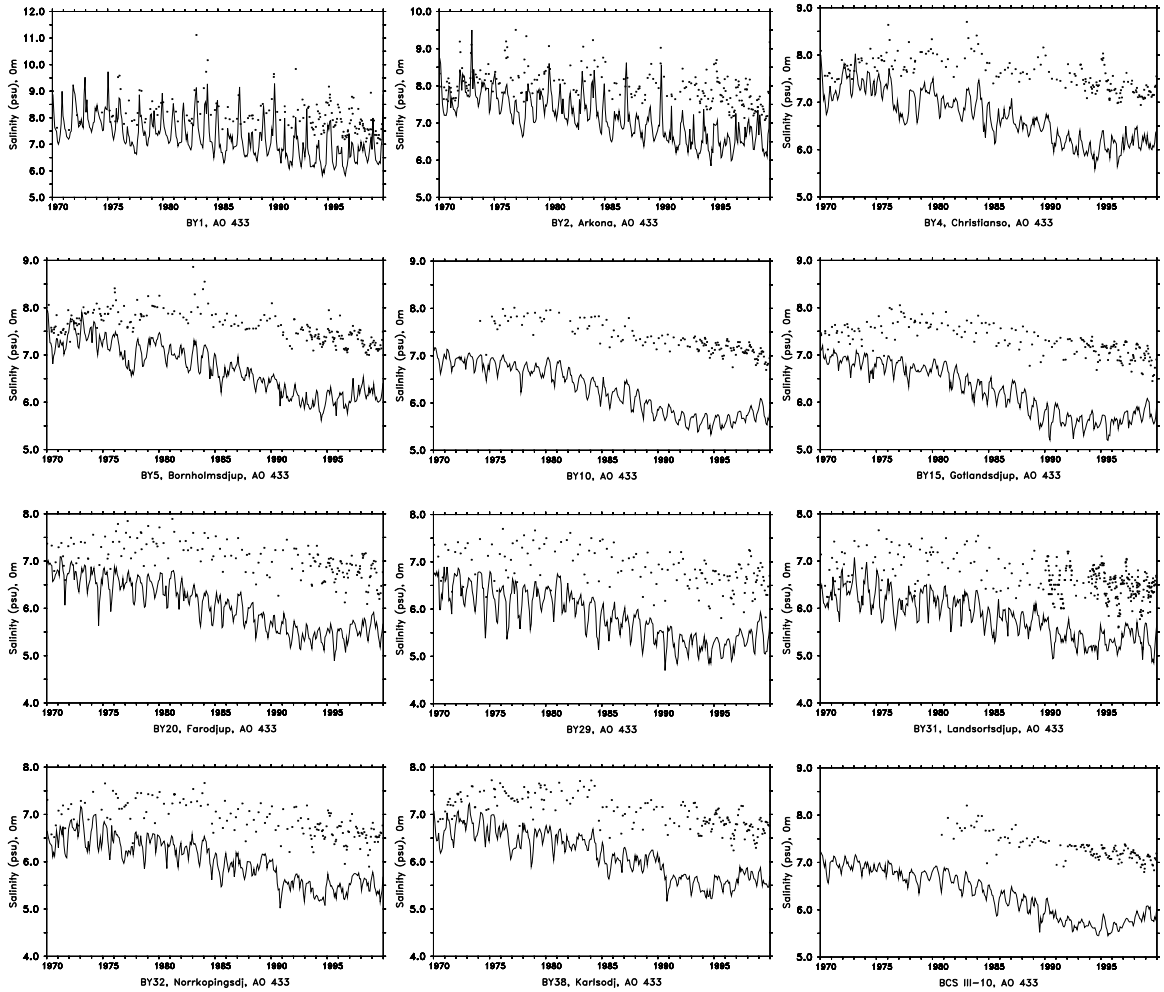

Figure 50: SSS series at stations throughout the model domain. Dots indicate measurements and the solid line model results.

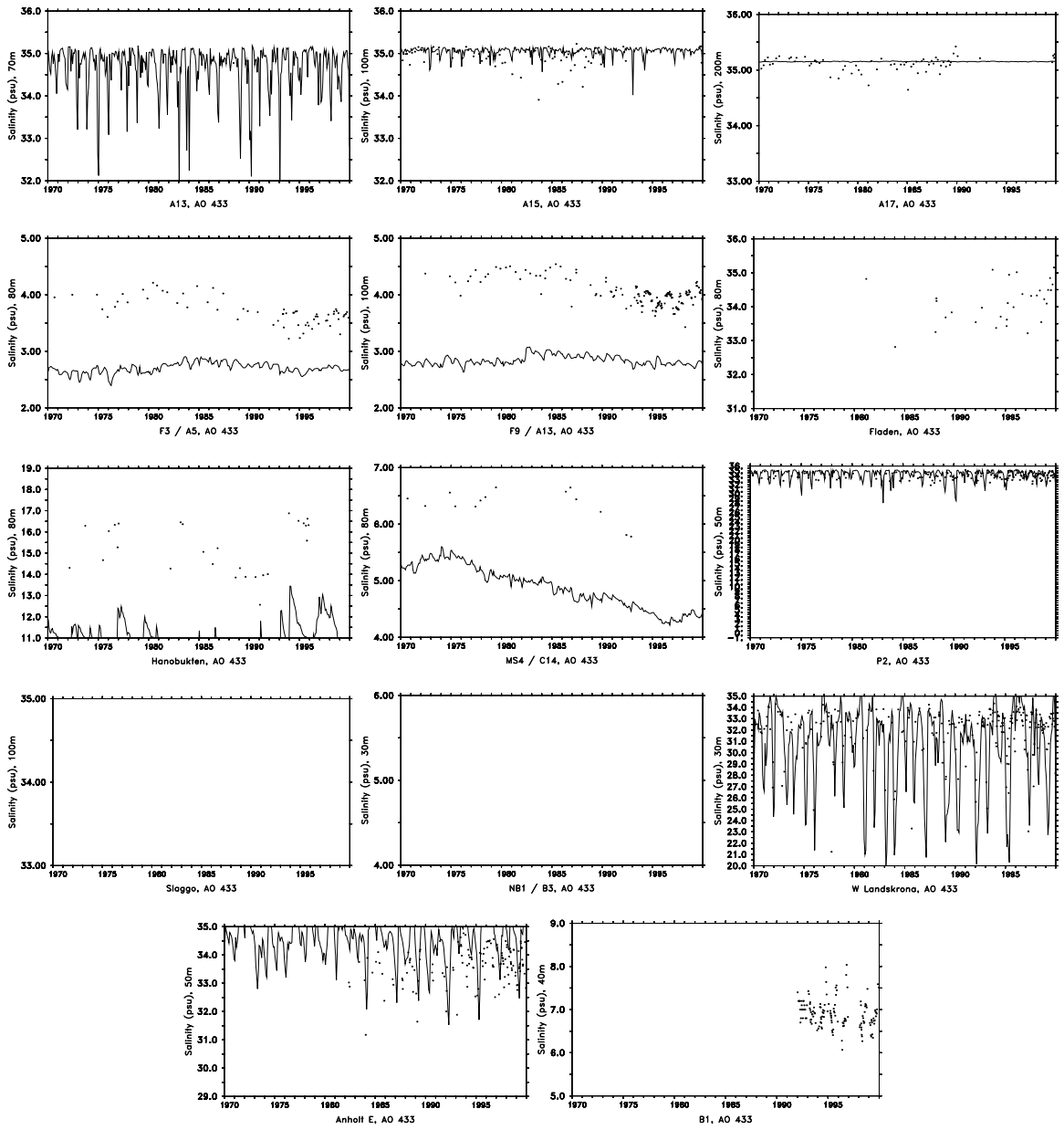

Figure 51: Salinity series at near bottom model levels for locations with observations. Dots indicate measurements and the solid line model results.

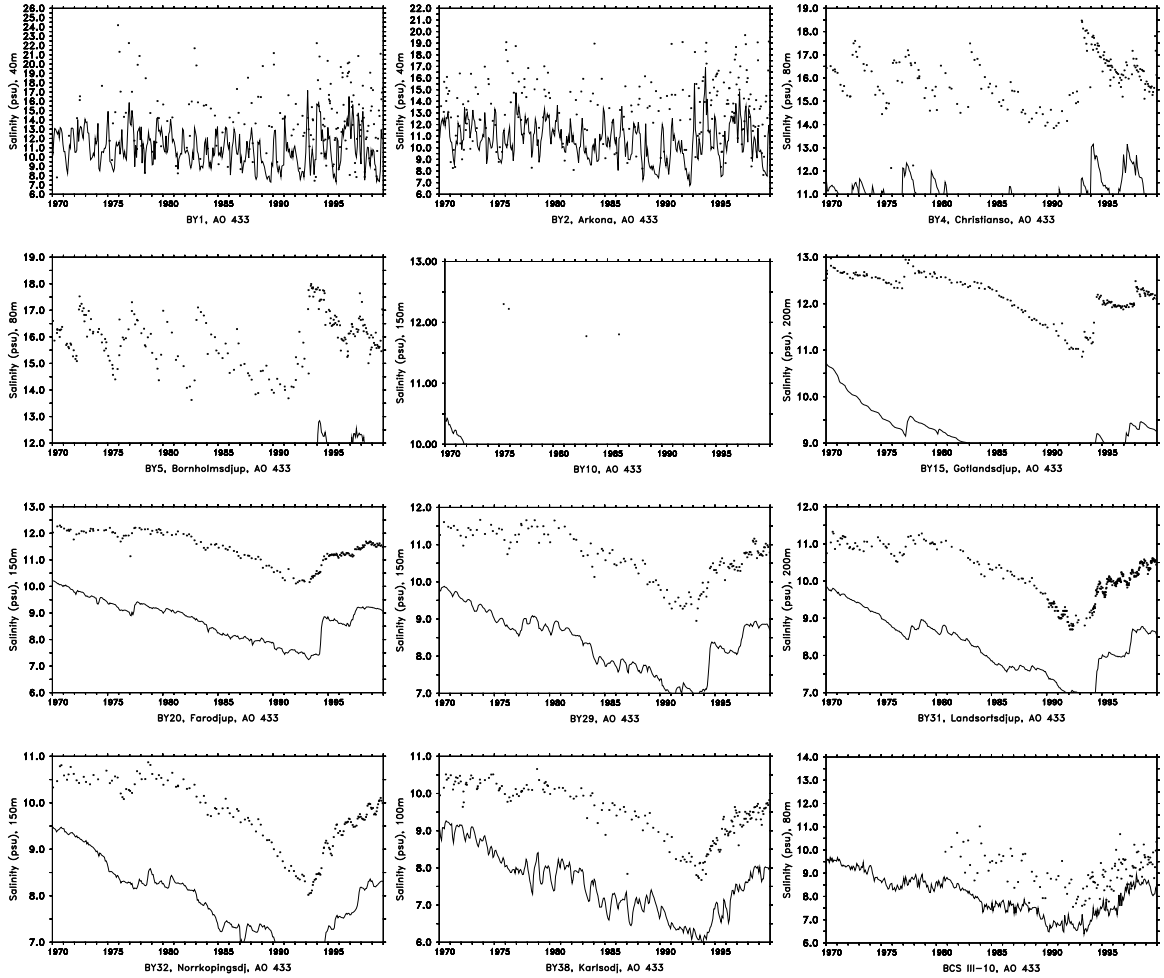

Figure 52: Salinity series at near bottom model levels for locations with observations. Dots indicate measurements and the solid line model results.

8 SMHI Publications

SMHI publish seven reportseries. Three of these, the R-series, are intended for international readers and are in most cases written in English. For the others the Swedish language is used.

Name of the series	**Published since**
RMK (Report Meteorology and Climatology)	1974
RH (Report Hydrology)	1990
RO (Report Oceanography)	1986
METEOROLOGI	1985
HYDROLOGI	1985
OCEANOGRAFI	1985
KLIMATOLOGI	2009

Earlier issues published in RO

1 Lars Gidhagen, Lennart Funkquist and Ray Murthy (1986)
Calculations of horizontal exchange coefficients using Eulerian time series current meter data from the Baltic Sea.

2 Thomas Thompson (1986)
Ymer-80, satellites, arctic sea ice and weather.

3 Stig Carlberg et al (1986)
Program för miljökvalitetsövervakning - PMK.

4 Jan-Erik Lundqvist och Anders Omstedt (1987)
Isförhållandena i Sveriges södra och västra farvatten.

5 Stig Carlberg, Sven Engström, Stig Fonselius, Håkan Palmén, Eva-Gun Thelén, Lotta Fyrberg och Bengt Yhlen (1987)
Program för miljökvalitetsövervakning - PMK. Utsjöprogram under 1986.

6 Jorge C. Valderama (1987)
Results of a five year survey of the distribution of UREA in the Baltic sea.

7 Stig Carlberg, Sven Engström, Stig Fonselius, Håkan Palmén, Eva-Gun Thelén, Lotta Fyrberg, Bengt Yhlen och Danuta Zagradkin (1988).
Program för miljökvalitetsövervakning - PMK. Utsjöprogram under 1987

8 Bertil Håkansson (1988)
Ice reconnaissance and forecasts in Storfjorden, Svalbard.

9 Stig Carlberg, Sven Engström, Stig Fonse-lius, Håkan Palmén, Eva-Gun Thelén, Lotta Fyrberg, Bengt Yhlen, Danuta Zagradkin, Bo Juhlin och Jan Szaron (1989)
Program för miljökvalitetsövervakning - PMK. Utsjöprogram under 1988.

10 L. Fransson, B. Håkansson, A. Omstedt och L. Stehn (1989)
Sea ice properties studied from the ice-breaker Tor during BEPERS-88.

11 Stig Carlberg, Sven Engström, Stig Fonselius, Håkan Palmén, Lotta Fyrberg, Bengt Yhlen, Bo Juhlin och Jan Szaron (1990)
Program för miljökvalitetsövervakning - PMK. Utsjöprogram under 1989.

12 Anders Omstedt (1990)
Real-time modelling and forecasting of temperatures in the Baltic Sea.

13 Lars Andersson, Stig Carlberg, Elisabet Fogelqvist, Stig Fonselius, Håkan Palmén, Eva-Gun Thelén, Lotta Fyrberg, Bengt Yhlen och Danuta Zagradkin (1991) Program för miljökvalitetsövervakning – PMK. Utsjöprogram under 1989.

14 Lars Andersson, Stig Carlberg, Lars Edler, Elisabet Fogelqvist, Stig Fonselius, Lotta Fyrberg, Marie Larsson, Håkan Palmén, Björn Sjöberg, Danuta Zagradkin, och Bengt Yhlen (1992)
Haven runt Sverige 1991. Rapport från SMHI, Oceanografiska Laboratoriet, inklusive PMK - utsjöprogrammet. (The conditions of the seas around Sweden. Report from the activities in 1991, including PMK - The National Swedish Programme for Monitoring of Environmental Quality Open Sea Programme.)

15 Ray Murthy, Bertil Håkansson and Pekka Alenius (ed.) (1993)
The Gulf of Bothnia Year-1991 - Physical transport experiments.

16 Lars Andersson, Lars Edler and Björn Sjöberg (1993)
The conditions of the seas around Sweden. Report from activities in 1992.

17 Anders Omstedt, Leif Nyberg and Matti Leppäranta (1994)
A coupled ice-ocean model supporting winter navigation in the Baltic Sea.
Part 1. Ice dynamics and water levels.

18 Lennart Funkquist (1993)
An operational Baltic Sea circulation model. Part 1. Barotropic version.

19 Eleonor Marmefelt (1994)
Currents in the Gulf of Bothnia. During the Field Year of 1991.

20 Lars Andersson, Björn Sjöberg and Mikaell Krysell (1994)
The conditions of the seas around Sweden. Report from the activities in 1993.

21 Anders Omstedt and Leif Nyberg (1995)
A coupled ice-ocean model supporting winter navigation in the Baltic Sea. Part 2. Thermodynamics and meteorological coupling.

22 Lennart Funkquist and Eckhard Kleine (1995)
Application of the BSH model to Kattegat and Skagerrak.

23 Tarmo Köuts and Bertil Håkansson (1995)
Observations of water exchange, currents, sea levels and nutrients in the Gulf of Riga.

24 Urban Svensson (1998)
PROBE An Instruction Manual.

25 Maria Lundin (1999)
Time Series Analysis of SAR Sea Ice Backscatter Variability and its Dependence on Weather Conditions.

26 Markus Meier[1], Ralf Döscher[1], Andrew, C. Coward[2], Jonas Nycander[3] and Kristofer Döös[3] (1999). RCO – Rossby Centre regional Ocean climate model: model description (version 1.0) and first results from the hindcast period 1992/93.

[1] Rossby Centre, SMHI [2] James Rennell Division, Southampton Oceanography Centre, [3] Department of Meteorology, Stockholm University

27 H. E. Markus Meier (1999)
First results of multi-year simulations using a 3D Baltic Sea model.

28 H. E. Markus Meier (2000)
The use of the $k - \varepsilon$ turbulence model within the Rossby Centre regional ocean climate model: parameterization development and results.

29 Eleonor Marmefelt, Bertil Håkansson, Anders Christian Erichsen and Ian Sehested Hansen (2000)
Development of an Ecological Model System for the Kattegat and the Southern Baltic. Final Report to the Nordic Councils of Ministers.

30 H.E Markus Meier and Frank Kauker (2002).
Simulating Baltic Sea climate for the period 1902-1998 with the Rossby Centre coupled ice-ocean model.

31 Bertil Håkansson (2003)
Swedish National Report on Eutrophication Status in the Kattegat and the Skagerrak OSPAR ASSESSMENT 2002

32 Bengt Karlson & Lars Andersson (2003)
The Chattonella-bloom in year 2001 and effects of high freshwater input from river Göta Älv to the Kattegat-Skagerrak area

33 Philip Axe and Helma Lindow (2005)
Hydrographic Conditions Around Offshore Banks

34 Pia M Andersson, Lars S Andersson (2006)
Long term trends in the seas surrounding Sweden. Part one - Nutrients

35 Bengt Karlson, Ann-Sofi Rehnstam-Holm & Lars-Ove Loo (2007)
Temporal and spatial distribution of diarrhetic shellfish toxins in blue mussels, Mytilus edulis (L.), at the Swedish West Coast, NE Atlantic, years 1988-2005

36 Bertil Håkansson
Co-authors: Odd Lindahl, Rutger Rosenberg, Pilip Axe, Kari Eilola, Bengt Karlson (2007)
Swedish National Report on Eutrophication Status in the Kattegat and the Skagerrak OSPAR ASSESSMENT 2007

37 Lennart Funkquist and Eckhard Kleine (2007)
An introduction to HIROMB, an operational baroclinic model for the Baltic Sea

38 Philip Axe (2008)
Temporal and spatial monitoring of eutrophication variables in CEMP

39 Bengt Karlson, Philip Axe, Lennart Funkquist, Seppo Kaitala, Kai Sørensen (2009)
Infrastructure for marine monitoring and operational oceanography

40 Marie Johansen, Pia Andersson (2010)
Long term trends in the seas surrounding Sweden
Part two – Pelagic biology

41 Philip Axe, (2012)
Oceanographic Applications of Coastal Radar

42 Martin Hansson, Lars Andersson, Philip Axe (2011)
Areal Extent and Volume of Anoxia and Hypoxia in the Baltic Sea, 1960-2011

43 Philip Axe, Karin Wesslander, Johan Kronsell (2012)
Confidence rating for OSPAR COMP

44 Germo Väli, H.E. Markus Meier, Jüri Elken (2012)
Simulated variations of the Baltic Sea halocline during 1961-2007

45 Lars Axell (2012)
BSRA-15 A Baltic Sea Reanalysis 1999-2004 (ej publicerad)

46 Martin Hansson, Lars Andersson, Philip Axe, Jan Szaron (2013)
Oxygen Survey in the Baltic Sea 2012 - Extent of Anoxia and Hypoxia, 1960 -2012

47 C. Dieterich, S. Schimanke, S. Wang, G. Väli, Y. Liu, R. Hordoir, L. Axell, A. Höglund, H.E.M. Meier (2013)
Evaluation of the SMHI coupled atmosphere-ice-ocen model RCA4-NEMO

48 R. Hordoir, B. W. An, J. Haapala, C. Dieterich, S. Schimanke, A. Höglund and H.E.M. Meier (2013)
BaltiX V 1.1 : A 3D Ocean Modelling Configuration for Baltic & North Sea Exchange Analysis

SMHI
Swedish Meteorological and Hydrological Institute
SE 601 76 NORRKÖPING
Phone +46 11-495 80 00 Telefax +46 11-495 80 01

ISSN 0283-1112